Arabian Journal of Geosciences (2022) 15: 270
https://doi.org/10.1007/s12517-022-09519-z

ORIGINAL PAPER

Coal petrology of Neogene low-rank coal in Mukah Coalfield, Sarawak, Malaysia: Implications for coal facies and paleodepositional reconstructions

Nor Syazwani Zainal Abidin[1,2,3] · Khairul Azlan Mustapha[4] · Wan Hasiah Abdullah[5] · Mohammed Hail Hakimi[6]

Received: 29 October 2021 / Accepted: 12 January 2022 / Published online: 27 January 2022

Abstract

A study using high-resolution macroscopy and microscopy was conducted on the Neogene Mukah coal in Sarawak, Malaysia, to describe the changes in the coal facies, peat development and its precursors, and depositional conditions of the peat/coal. Eight coal seams from three boreholes (MC05, MC12, MC01) were analyzed. Bright, banded bright, banded dull, and dull coal lithotypes, with a predominance of the brighter lithotypes, were identified and primarily attributed to increases in huminite content and decreases in liptinite and mineral matter contents. Coals were characterized by high huminite (70.3%–91.9%), moderate liptinite (4.0%–26.3% mmf), minor inertinite (1.4%–5.9% mmf), and argillaceous mineral matter (0.0%–50.6%). Clarite (3.5%–88.7%) was observed to be the most predominant microlithotypes with carbominerite content ranging from 0.0% to 67.9%. The complete succession from topogenous to ombrogrenous peat evolution was identical between the eight coal seams, and temporary development of rheotrophic–ombrotrophic mires was suggested. The basal section of coal bench was dominated by humodetrinite/liptinite-rich coal or humocollinite/mineral matter-rich coal, whereas the middle section was characterized by humotelinite- and humocollinite/liptinite-rich coal and overlain by humotelinite-rich coal. The Mukah coal was suggested to have been deposited in a coastal floodplain within a (mainly) upper–lower delta plain setting more prone to telmatic coal facies.

Keywords Facies modeling · Lithotype · Ombrotrophic mires · Paralic coal · Paleomire · Telmatic

Responsible Editor: Domenico M. Doronzo

✉ Khairul Azlan Mustapha
azlan_0401@um.edu.my; azlan.geo@gmail.com

[1] Department of Geology, Faculty of Science, University of Malaya, 50603 Kuala Lumpur, Malaysia

[2] Geoscience Department, Faculty of Science and Information Technology, Universiti Teknologi PETRONAS, Perak 32610 Bandar Seri Iskandar, Malaysia

[3] Southeast Asia Clastic & Carbonate Research Laboratory (SEACARL), Institute of Hydrocarbon Recovery for Enhanced Oil Recovery, Universiti Teknologi PETRONAS, 32610 Bandar Seri Iskandar, Perak, Malaysia

[4] Department of Geology, Faculty of Science, University of Malaya, 50603 Kuala Lumpur, Malaysia

[5] Geological Society of Malaysia, c/o Department of Geology, University of Malaya, 50603 Kuala Lumpur, Malaysia

[6] Geology Department, Faculty of Applied Science, Taiz University, 6803 Taiz, Yemen

Introduction

The central region of Sarawak, comprising the Mukah–Balingian areas, forms the onshore region of the extensively studied Balingian Province, which contains economically important coal seams considered to be the most prolific producers of humic coal in Malaysia (e.g., Abdullah, 1997a; Abdullah, 1997b; Abdullah, 2002; Sia and Abdullah 2012b; Hakimi et al. 2013; Sia et al. 2014) (Fig. 1a). Previously, studies on the Mukah–Balingian areas were limited to general geological and paleontological research (Visser and Crew 1950; Liechti et al. 1960; Wolfenden 1960), the quality and re-estimation of coal reserves (Chen 1986), and lithostratigraphy (De Silva 1986). However, after 2000, studies on petrographic and geochemical coal (Sia and Dorani 2000; Sia and Abdullah 2012b; Hakimi et al. 2013), coalbed methane (Irwan et al. 2012), palynology and paleodepositional environments (Sia et al. 2014; Murtaza et al. 2015), the concentration of coal-related minor elements and trace components (Sia and Abdullah 2011, 2012a), characteristics

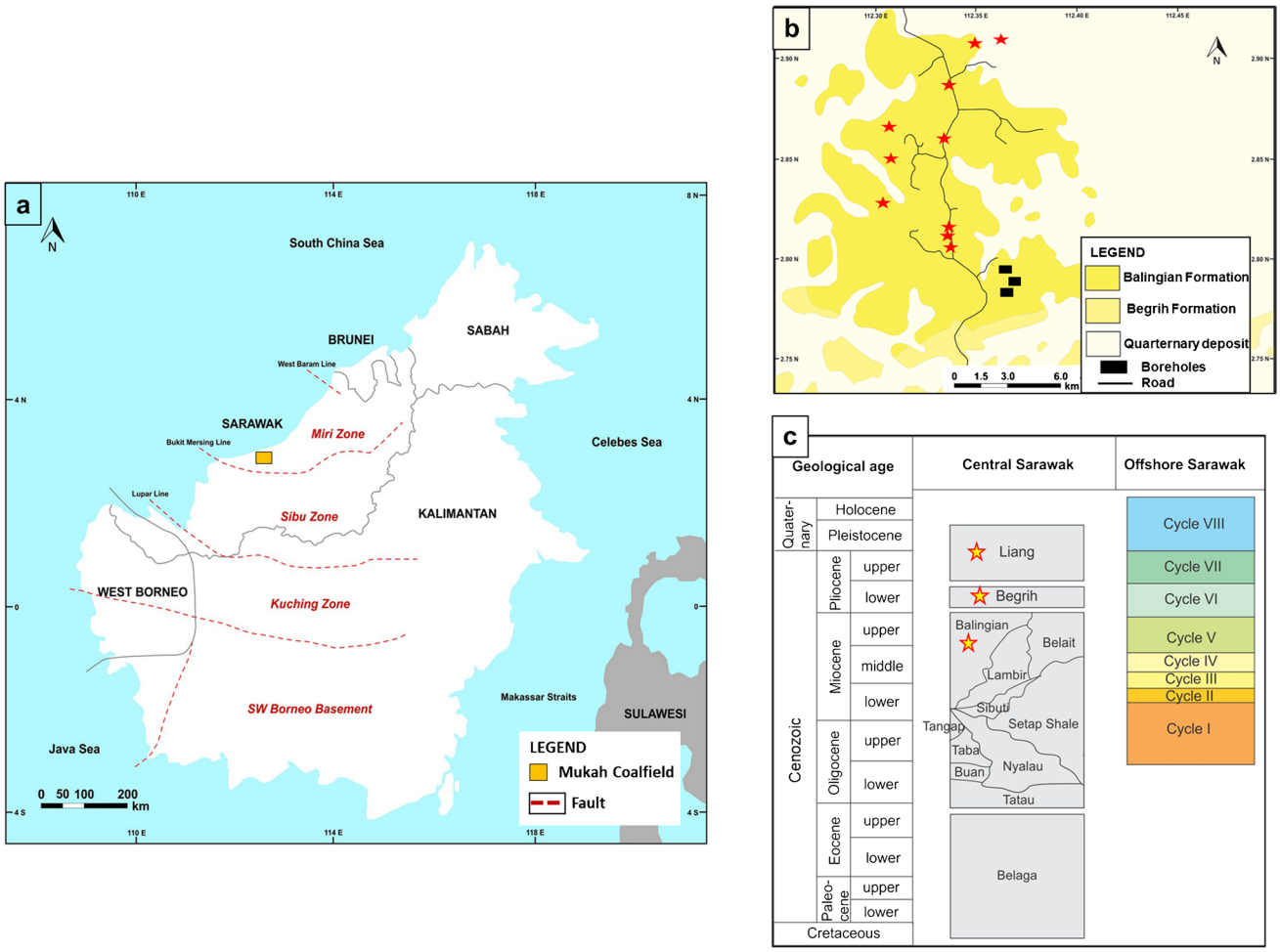

Fig. 1 (a) Geological map of Borneo (modified from Widodo et al., 2010). The geology of the (b) Mukah Coalfield and borehole samples. Note the sampling points of the previous work by Sia and Abdullah (2011), Sia et al. (2014), Hakimi et al. (2013), and Murtaza et al. (2018). (c) The stratigraphic chart of Central Sarawak. The Balingian, Begrih, and Liang Formations are only exposed in the Mukah–Balingian areas (modified from Mazlan 1999)

of reservoir (Nugraheni et al. 2014), paleogeographic evolution (Ramkumar et al. 2018; Murtaza et al. 2018; Hennig-Breitfeld et al. 2019), paleovegetation and paleoclimates (Sia et al. 2019), and sequence biostratigraphic frameworks (Morley et al. 2021) were performed in this area.

The coal formation currently being investigated is from the Mukah Coalfield, Sarawak (Fig. 1b), located in the low-lying coastal plain between the Mukah and Balingian Rivers, and covering an area of ~ 300 km^2. These coal-bearing sequences are Cenozoic in age (Wolfenden 1960) and were deposited between the Early to Middle Miocene Balingian Formation (Sia et al. 2014; Murtaza et al. 2018) that underlies the coalfield and, in turn, is unconformably overlain by the Late Miocene to Early Pliocene Begrih Formation (Wolfenden 1960; Liechti et al. 1960; Hutchison 2005; Murtaza et al. 2018) (Fig. 1c). Contact between these two formations is marked by a wedge of basal conglomerate called the Begrih Conglomerate (Wolfenden 1960; Sia and Dorani 2000). The offshore equivalent to the onshore stratigraphy is believed to be between Cycles II and V of the Sarawak Basin (Fig. 1c) (Mazlan 1999).

The foraminifera analyses of the Balingian Formation have demonstrated a predominance of *Ammodiscus* sp., *Glomospira* sp., *Haplophragmoides* sp., and *Trochammina* sp., indicating a brackish water environment (Wolfenden 1960; Liechti et al. 1960; Hutchison 2005). The sub-environments of Balingian Formation are defined by tide-influenced channels and brackish facies in the basal section, estuaries in the central section, and upper and lower coastal plains in the top section (Murtaza et al. 2018).

Previously, studies on the coal petrology of the Balingian Formation have indicated that Mukah coal is characterized by high amounts of detrohuminite and lignite to subbituminous B in rank, high total moisture, low total sulfur content, and low ash yield (Sia et al. 2014). Furthermore, the low sulfur concentration and palynomorph assemblages

recovered from the Mukah coal seams indicate that the coal-forming peat was deposited in freshwater mires (Sia et al. 2014). Palynological studies on Mukah coal have indicated an abundance of arboreal pollen assemblages of *Casuarina* sp. and *Dacrydium* sp., suggesting the presence of Kerangas vegetation and Kerapah-type peat swamps in the precursor mires (Sia et al. 2014).

This study is the first attempt to utilize high-resolution macroscopic and microscopic analyses of the Neogene coal developed in the Mukah Coalfield. This study applies coal lithotype, maceral, and microlithotype analyses that primarily emphasize the intra-seam and whole seam variations of the coal. Based on organic petrography, the vertical lithotype variations combined with data on the petrographic compositions, characteristics of the seams, and facies modeling are used to describe the coal facies, changes in the peat development and its precursors, and dynamics of the depositional conditions for the Mukah coal.

Sampling and methods

Three 50-m-deep mining boreholes were obtained from the Mukah Coalfield; their coordinates were provided by the mining company and taken based on the south orientation of the sedimentary dipping and east–west strike orientation. The cores were analyzed and described for litholofacies, coal seams, and coal lithotypes. The boreholes and their coal seams were named MC05 (05/01, 05/02, 05/03), MC12 (12/01), and MC01 (01/01, 01/02, 01/03, 01/04) from the base to the top of the coal-bearing sequence (Fig. 2).

The coal lithotype analysis on each of the coal seams was performed under high-resolution observation with a thickness of 2 cm was used for the analysis. Characterization of the coal lithotypes from the base to the top of the seams on a macroscopic scale was recorded based on the brightness system proposed by Diessel (1965) and Anon (1981). In total, for petrographic analysis, 45 coal samples from each coal lithotype were prepared. The coal samples were crushed to 18mesh size (< 1 mm size particles). The polished particulate coal mounts were prepared using a mixture of cold mounting Serifix-resin and hardener without pressure (Taylor et al. 1998), and the pellets were mounted perpendicular to the bedding. The organic petrographic characteristics were described under a plane-polarized reflected light using a Leica DM 6000 M microscope and Leica CTR6000 photometry system equipped with fluorescence illuminators.

Petrographic composition was determined by maceral and combined maceral–microlithotype analyses, as described by Taylor et al. (1998), Hower and Wagner (2012), International Committee for Coal and Organic Petrology (ICCP) for huminite (Sýkorová et al. 2005), liptinite (Pickel et al. 2017), and inertinite (ICCP 2001) nomenclature. The quantitative and qualitative analyses of the huminite, liptinite, and inertinite macerals were determined at the cross-hair of the field reticule and the maceral assemblage, or microlithotypes, within a radius of 25microns from the centre (vol. %). Combined two-digit maceral and one-digit microlithotype codes were used (Hower and Wagner 2012). Here, 1,000 points with a gap of 50 µm between each point were counted on each polished sample, while the distances between points and the lines of points were 0.5 mm. The block was placed at an angle so that continuous counting within the lithotype did not land on the same band, the megascopically-identifiable section within the coal seam. For this study, a modification was necessary because the studied coal was of low rank. Therefore, vitrinite submacerals were substituted by huminite submacerals (i.e., humotelinite, humodetrinite, and humocollinite). The combined maceral–microlithotype data were included in a modified Excel spreadsheet (Hower and Wagner 2012) that was extended from the previous simplified versions to accommodate the ICCP macerals (International Coal and Organic Petrology Committee 1998; Taylor et al. 1998).

Then, the vertical coal logs and their compositional variations and associated lithofacies with the coal seam and coal facies data (Mukhopadhyay 1986; Singh and Singh 1996; Lamberson et al. 1991; Amijaya and Littke 2005; Calder et al. 1991; Hacquebard and Donaldson 1969; Singh et al. 2010) were used to interpret the paleofacies, paleomires, and depositional environments, supported by the ash yield evaluation (ASTM D5142 2009).

Results

Macroscopic description and interpretation of coal-bearing strata

The lowermost section (MC05) of the analyzed boreholes (Fig. 2, 94–127 m) demonstrated that the thick coal seams, carbonaceous mud, and organic-rich mudrocks at the base were interpreted as coastal swamp facies. The coarsening upward trend indicated the gradual decrease in growth of the peat-forming environment into a more clay-rich and sand-rich deposition. This trend suggested an increase in depositional energy within a shallowing setting, starting with flood plain deposits and followed by fluvial channel fills. The middle section (MC12) (Fig. 2, 50–94 m) of the Balingian Formation demonstrated that the fining upward trend reflected the change from a sand-dominated deposition at the base, followed by the abandonment of sand-rich lithologies into more clay-rich lithologies and a peat-forming environment, thus indicating an upward decrease in the depositional energy from a fluvial channel fill to a flood plain fill. Borehole MC01, which represented the topmost

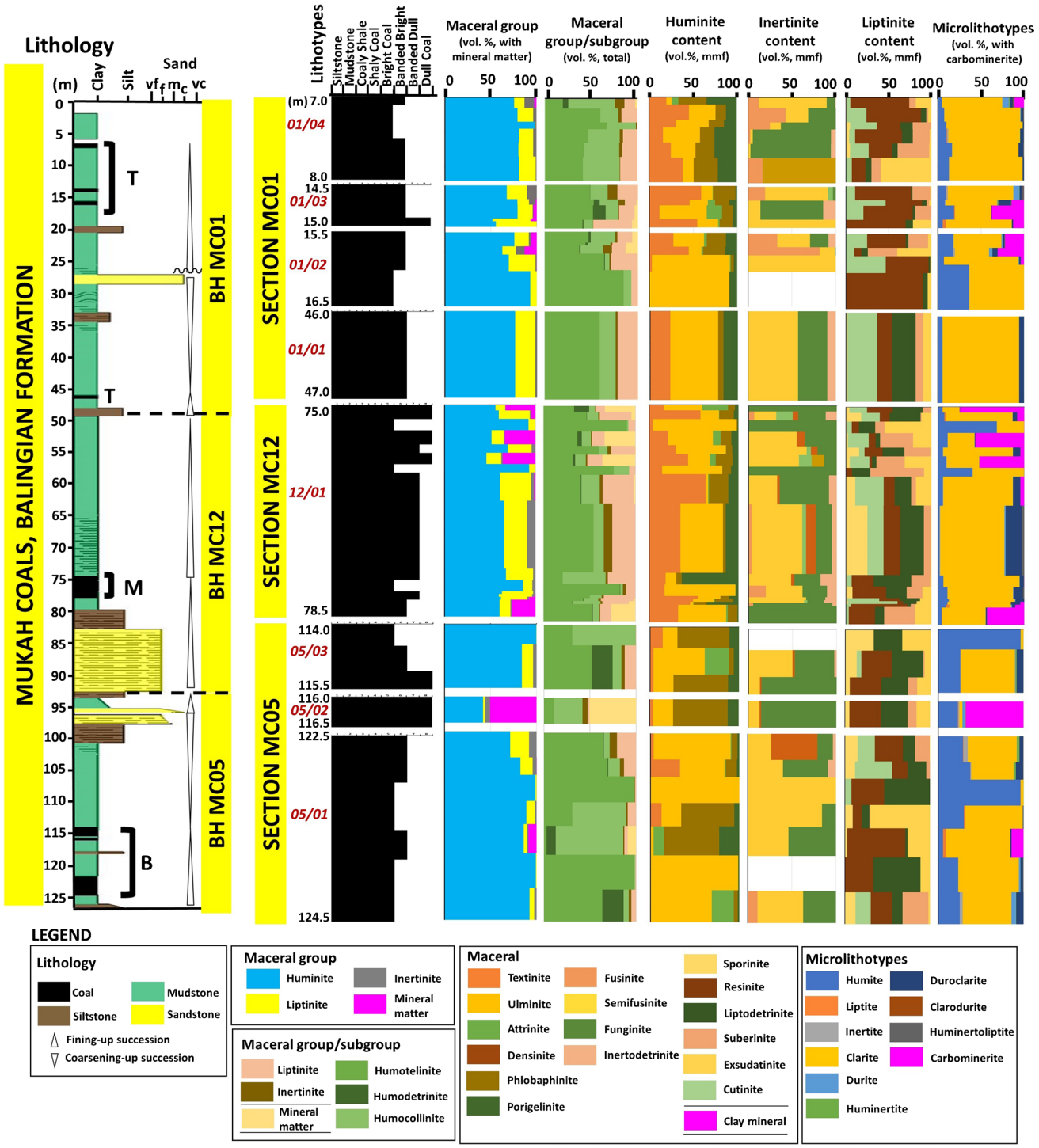

Fig. 2 Complete vertical profile of the whole seams and intra-seams showing the upward compositional changes in lithotypes, macerals, submacerals, mineral matter, and microlithotypes for the studied Mukah coal. Note that seams within the coal sections are labeled, e.g., 05/01

section (Fig. 2, 3–50 m), was generally characterized by a top section that displayed composite beds of fining upward units and was capped by a mudstone facies and overlain by thin coal layers. The hydraulic energy was suggested to be low and hence interpreted as fluvial-dominated floodplain fills that reflected the gradual overgrowth and changed into a peat-forming environment from an active channel setting.

The coal-bearing strata of the Balingian Formation were dominated by mudstones with coarser-grained sandstone, mainly at 80–100 m in depth, whereas coal seams occurred

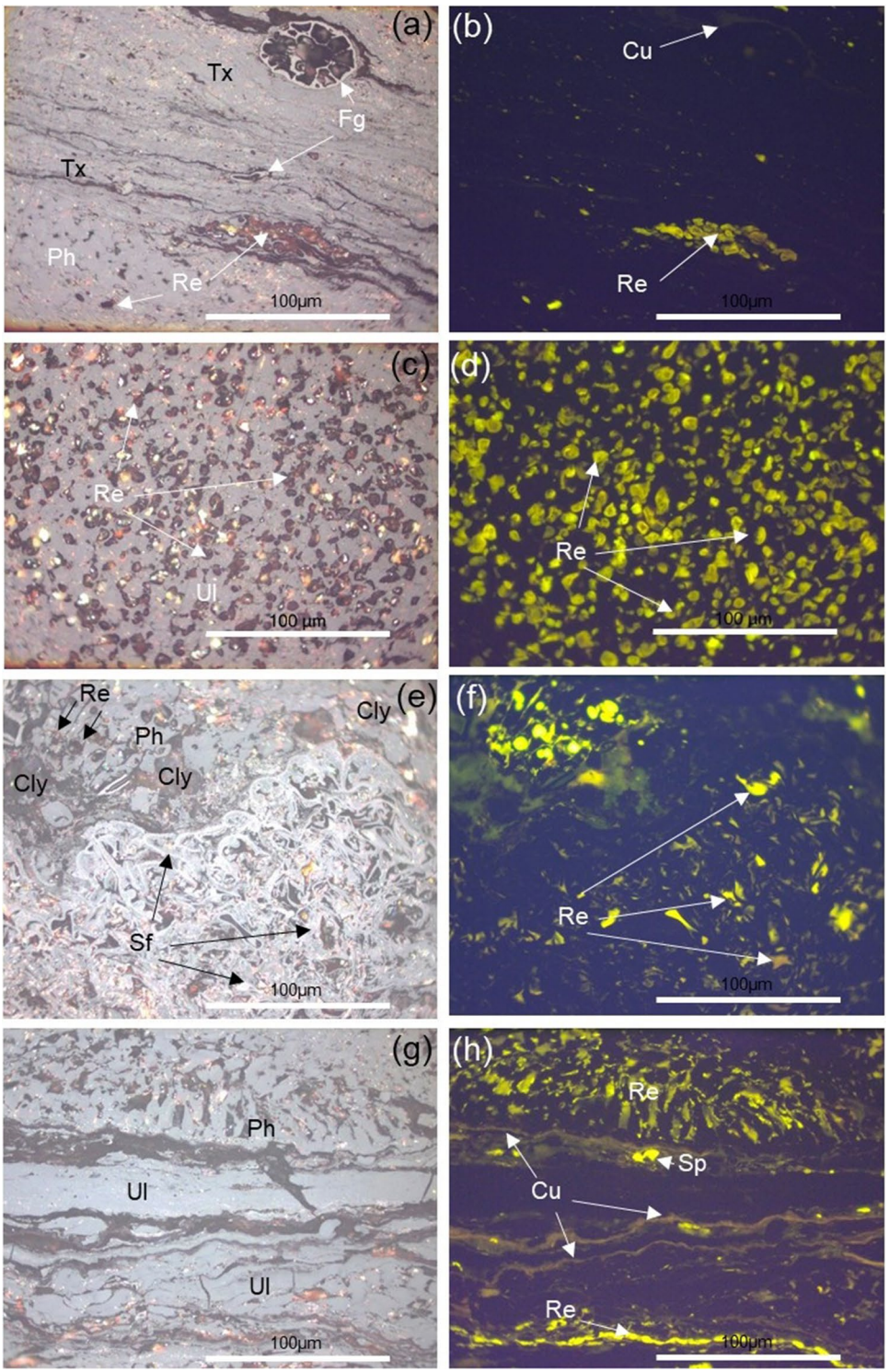

Fig. 3 Photomicrographs of (a) banded bright coal (BBC), showing the dominant presence of humotelinite submacerals (textinite, Tx); reflected light, (b) similar view of figure (a) under uv light, (c) bright coal (BC), showing predominant of ulminite (Ul) with cavities filled with resinite; reflected light (d) similar view of figure (c) under uv light, (e) dull coal (DC), showing the presence of semifusinite (Sf) sandwiching resinite (Re), while resinite filled the cellular cavities of textinite (Tx) at left edge and clay minerals were dispersed; reflected light (f) similar view of figure (e) under uv light, (g) banded dull coal (BDC), showing the association of macerals consisting of bands of huminite and liptinite macerals constituting more than 95%; reflected light (h) similar view of figure (g) under uv light

in the middle and lowermost parts of the formation. Generally, the formation in this study was interpreted to be deposited in a low-lying coastal plain environment with an overall fluvial influence. However, variation in the deposition environment may have occurred in different places in the Mukah Coalfield.

Characteristics of the coal

Coal lithotypes

A total of eight seams were identified from the base to top of the coal-bearing sequences. The thickness of the seams

ranges from 0.5 to 3.5 m (Fig. 2). Four lithotypes were observed: bright coal, banded bright coal, banded dull coal, and dull coal (Fig. 2 and 3). From the coal log, the vertical profile (Fig. 2) showed a predominance of bright coal (> 70%) in seam MC05, with the overall brightness pattern of the seams showing an increasing trend toward the top seam. Brighter lithotypes predominated in the basal (05/01) and top (05/03) seam, while dull coals prevailed in the middle seams (05/02). However, the middle section MC12 had a predominance of the dull coal lithotype (> 70%) and shows a decrease in brightness represented by dull lithotypes toward the top of the seam. Banded dull lithotypes with thicknesses up to 1.5 m are mostly found in the middle part of the seam. In contrast, brighter lithotypes, specifically bright and banded bright, with thicknesses of less than 0.5 m prevailed toward the base of the seam. Moreover, the topmost section MC01 was primarily characterized by a predominance of brighter coal as the banded bright lithotype (> 70%). The bright coals were found at the middle and top part of the section with thicknesses up to 0.5 m. Furthermore, dull coal was found in the middle part (seam 01/03) with less than 0.5 m thickness. No clastic bands were observed within the coal seams. In general, it is suggested that the upward trend of the Mukah coal's brightness increases in the sections MC05 and MC01, whereas a "dulling-up" trend characterizes section MC12 from the base to top of the coal intervals (Fig. 2).

Maceral composition of the coal

Table 1, Fig. 3a–h, and Fig. 4a–b show the overall compositions of various macerals and mineral matter content in range and average (avg.) as total (vol. %) and mineral-free basis (vol. %, mmf) of the analyzed coals. The Mukah coal from the Balingian Formation was dominated by the huminite group (70.3%–91.9% mmf), with high humotelinite (22.2%–62.1% mmf), moderate humocollinite (10.0%–62.6% mmf), and low humodetrinite (3.1%–28.1% mmf) (Table 1, Fig. 4a, d). A low-to-moderate occurrence of liptinite (4.0%–26.3% mmf) was reported with resinite being the most dominant, ranging in average concentration from 1.5% to 11.4% (mmf), followed by cutinite (0.0%–7.7% mmf), liptodetrinite (1.0%–6.1% mmf), suberinite (0.1%–4.9% mmf), exsudatinite (0.5%–4.9% mmf), and sporinite (0.0%–2.3% mmf) (Table 1, Fig. 4a, e). A very minor amount of inertinite (1.4%–5.9% mmf) was observed (< 10%).

The mineral matter concentration in the Mukah coal demonstrated low-to-moderate amounts with the average amount ranging from 0.0% to 50.6%. The highest amount of argillaceous mineral matter was observed in MC05-middle. All samples have trace amounts of pyrite, thus were not recorded in this study. The inertinite–huminite/vitrinite (IV) factor was low (mean 3.7) for the Mukah coal (Table 1).

Maceral composition of lithotypes

In general, petrographic analyses demonstrated a good relationship between the composition of the maceral groups and lithotypes of the Mukah coal (Fig. 4c) on an mmf basis. The huminite concentration increased from the duller lithotype to the bright coal lithotype (Fig. 4c). The bright coal lithotype was characterized by a high huminite concentration of > 80 vol.%; humotelinite and humocollinite were mostly reported in the bright coal, with the former being predominant (Fig. 4d). Humodetrinite was less common in the bright coal. The banded bright, banded dull, and dull lithotypes had an abundance of huminite macerals, mostly ranging from 60 to 85%, with a predominance of humotelinite. However, humocollinite was reported in moderate amounts (10%–50%), whereas humodetrinite occurs in amounts < 30% in these lithotypes (Fig. 4d). Based on the liptinite distributions (vol. %, mmf) in Fig. 4e, the concentrations of resinite, cutinite, and liptodetrinite varied in all coal lithotypes. However, two trends were observed in the banded bright coal lithotype. Resinite was found high, with a low concentration of liptodetrinite and moderate amount of cutinite macerals. In comparison, cutinite, liptodetrinite, and resinite were reported in high amounts ranging from 20 to 50% (Fig. 4e). Moreover, inertinite was reported in low concentrations, with fusinite, semifusinite, funginite, and inertodetrinite were reported in various amounts in all lithotypes (Fig. 2). Regarding the mineral matter, comprising mostly clay minerals (vol. %), the concentration increased from the bright lithotype to the duller lithotype (Fig. 4f). The dull coal lithotype was characterized by a higher amount of clay mineral that ranged from 30 to 55%. It is suggested that the dullness of lithotypes was primarily attributed to the presence of liptinite and mineral matter, while the brightness in lithotypes increases with increasing huminite content (Fig. 4e–f).

To summarize, maceral distributions (Fig. 2) demonstrated huminite to be most dominant from the lowermost to topmost sections of the Mukah coal, followed by liptinite and inertinite, with mineral matter primarily found in the layers containing a duller lithotype. Humotelinite, resinite, and semifusinite were the most common submacerals throughout the sections.

Microlithotype composition of the coal

The microlithotype groups observed in the Mukah coal from the Balingian Formation were illustrated based on their average composition (vol.%, Fig. 2) and carbominerite-free basis (cmf, vol.%) from each coal seam (Table 2). The bimaceral group was indicated as the most dominant in all samples, in which clarite predominates throughout the sections, ranging from 3.5% to 88.7%

Table 1 Petrographic compositions showing the range and average (avg.) values of the coal sections in the Mukah coal on a total (vol.%), and mmf basis (vol.%). The IV factors, correlation coefficients of the maceral groups (mineral free) and minerals, and maceral indices for the coal facies (e.g., TPI-GI and GWI-VI) (Mukhopadhyay 1986; Singh and Singh 1996; Lamberson et al. 1991; Calder et al. 1991) are also shown

Coal Section	MC 01						MC 12						MC 05						Avg	Avg
Seams	01/04	01/02–01/03	01/01	01/04	01/02–01/03	01/01	T	M	B	T	M	B	05/03	05/02	05/01	05/03	05/02	05/01		
	(vol. %)			(vol. %, mmf)			(vol. %)			(vol. %, mmf)			(vol. %)			(vol. %, mmf)			(vol. %)	(vol. %, mmf)
Textinite	12.8–46.7	0.0–39.8	17.5	12.8–46.7	0.0–39.8	17.5	3.8–34.3	13.6–38.7	12.4–34.4	3.8–36.0	13.6–39.3	12.4–34.4	3.2–14.1	1.5	0.0–27.4	3.2–14.1	3.1	0.0–27.4	1.5–26.2	3.1–28.1
Ulminite	4.6–34.3	8.9–84.8	41.6	4.7–34.3	8.9–84.8	41.6	12.4–86.9	1.7–62.8	2.4–68.4	13.0–86.9	1.7–62.8	2.5–68.4	16.6–48.6	9.5	2.7–98.7	16.6–48.6	19.1	3.0–98.7	9.5–55.1	19.1–55.2
Humotelinite	19.5–70.1	37.2–84.8	59.1	20.0–70.1	42.9–84.8	59.1	33.3–90.7	31.3–76.3	20.5–83.3	48.9–90.7	41.0–76.3	20.5–83.3	30.7–51.8	11.0	2.9–98.7	30.7–51.8	22.2	3.2–98.7	11.0–61.1	22.2–62.1
Attrinite	0.0–5.8	0.0–13.7	0.0	0.0–5.9	0.0–14.2	0.0	0.0–16.1	0.1–3.1	0.0–1.1	0.0–24.1	0.1–4.9	0.0–1.5	0.0–22.9	0.0	0.0–22.8	0.0–22.9	0.0	0.0–22.8	0.0–11.5	0.0–11.5
Densinite	0.0	0.0	0.0	0.0	0.0	0.0	0.0	0.0	0.0	0.0	0.0	0.0	0.0	0.0	0.0	0.0	0.0	0.0	0.0	0.0
Humodetrinite	0.0–5.8	0.0–13.7	0.0	0.0–5.9	0.0–14.2	0.0	0.0–16.1	0.1–3.1	0.0–1.1	0.0–24.1	0.1 -4.9	0.0 -1.5	0.0–22.9	0.0	0.0–22.8	0.0–22.9	0.0	0.0–27.4	0.0–11.5	3.1–28.1
Phlobaphinite	9.4–24.4	0.0–17.3	4.7	9.4–25.0	0.0–18.2	4.7	0.8–9.6	8.7–13.2	0.7–12.3	0.8–10.1	9.0–13.7	0.7–12.4	4.5–58.4	25.8	0.0–53.6	4.5–58.4	52.2	0.0–58.9	4.7–31.5	4.7–52.2
Porigelinite	4.2–26.0	1.3–9.6	12.4	4.2–26.7	1.3–10.2	12.4	0.9–4.8	2.9–7.6	0.7–42.8	0.9–4.8	4.6–7.6	0.9–42.8	4.9–10.6	5.1	0.0–19.6	4.9–10.6	10.4	0.0–21.5	3.0–15.6	3.6–15.7
Humocollinite	18.3–50.4	5.0–26.1	17.1	18.3–51.7	5.0–28.0	17.1	1.7–12.7	11.7–20.1	2.6–47.0	1.7–15.4	16.6–20.4	2.6–47.0	9.4–69.0	30.9	0.0–73.2	9.4–69.0	62.6	0.0–80.3	8.2–39.2	10.0–62.6
Huminite group	72.5–88.7	51.9–93.0	76.1	72.5–88.7	55.4–93.0	76.1	51.6–92.4	46.1–93.1	59.6–86.2	62.5 -92.4	61.9–93.1	60.2–86.2	84.1–99.7	41.9	71.3–99.2	84.1–99.7	84.8	71.3–99.2	41.9–91.9	70.3–91.9
Fusinite	0.0–1.5	0.0–7.8	0.0	0.1–15	0.0–9.0	0.0	0.0	0.0	0.0–0.7	0.0–0.1	0.0	0.0–0.7	0.0	0.0	0.0–0.3	0.0	0.0	0.0–0.3	0.0–1.3	0.0–1.4
Semifusinite	0.1–8.1	0.0–7.5	1.2	0.0–8.3	0.0–7.5	1.2	0.0–2.7	0.0–1.1	0.0–5.3	0.0–2.7	0.0–1.3	0.0–5.3	0.0–1.8	0.7	0.0–2.2	0.0–1.8	1.5	0.0–2.2	0.6–1.6	0.8–2.3
Micrinite	0.0–0.1	0.0	0.0	0.0–0.1	0.0–0.6	0.0	0.0–0.3	0.0–0.2	0.0–0.4	0.0–0.3	0.0–0.3	0.0–0.4	0.0	0.0	0.0–0.0	0.0	0.0	0.0–0.0	0.0–0.1	0.0–0.1
Macrinite	0.0	0.0	0.0	0.0	0.0	0.0	0.0–0.3	0.0	0.0–0.1	0.0–0.3	0.0–0.1	0.0–0.1	0.0	0.1	0.0–4.3	0.0–0.1	0.2	0.0–4.3	0.0–1.6	0.0–1.1
Secretinite	0.0–0.5	0.0	0.0	0.0–0.5	0.0	0.0	0.0	0.0–0.2	0.0	0.0	0.0–0.3	0.0	0.0	0.0	0.0–0.0	0.0	0.0	0.0–0.0	0.0–0.1	0.0–0.1
Funginite	0.0–3.1	0.0–4.9	0.7	0.0–3.1	0.0–5.0	0.7	0.1–0.9	0.1–1.9	0.5–1.8	0.1–0.9	0.1–1.9	0.5–1.9	0.0–1.6	4.7	0.0–2.1	0.0–1.6	9.6	0.0–2.2	0.1–4.7	0.3–3.3
Inertodetrinite	0.0–0.3	0.0–1.0	0.2	0.0–0.3	0.0–1.0	0.2	0.0	0.1–0.3	0.0–0.5	0.0–0.2	0.0–0.3	0.0–0.5	0.0	0.0	0.0–0.4	0.0–0.1	0.0	0.0–0.4	0.0–0.3	0.0–0.3
Inertinite group	0.6–10.4	0.0–10.5	2.0	0.6–10.7	0.0–11.1	2.0	0.1–1.6	0.1–3.3	1.2–9.2	0.1–1.7	0.1–3.4	1.6–9.2	0.0–3.7	5.5	0.0–8.2	0.0–3.7	11.2	0.0–8.2	1.4–5.5	1.4–5.9
Sporinite	0.0–0.8	0.0–0.2	0.4	0.0–0.8	0.0–0.2	0.4	0.3–6.1	0.0–3.7	0.0–6.3	0.1–6.4	0.0–3.8	0.0–6.3	0.1–1.6	0.1	0.0–3.0	0.1–1.6	0.2	0.0–3.0	0.0–2.2	0.0–2.3
Cutinite	0.1–3.9	0.0–13.4	7.7	0.1–3.9	0.0–13.4	7.7	0.4–7.4	0.0–11.4	0.0–21.3	0.4–7.8	0.0–11.5	0.0–12.8	0.0–0.7	0.0	0.0–5.7	0.0–0.7	0.0	0.0–5.7	0.0–7.7	0.0–7.7
Resinite	0.1–11.0	1.3–29.0	3.7	0.1–11.0	1.5–31.0	3.7	0.6–5.5	0.5–4.4	3.6–19.1	0.6–5.5	0.5–4.5	2.4–20.6	0.0–4.3	0.7	0.3–6.7	0.0–4.3	1.5	0.3–6.7	0.7–11.0	1.5–11.4
Alginite	0.0	0.0	0.0	0.0	0.0	0.0	0.0	0.0	0.0	0.0	0.0	0.0	0.0	0.0	0.0	0.0	0.0	0.0	0.0	0.0
Liptodetrinite	0.0–3.1	0.3–3.6	6.1	0.0–3.1	0.3–3.8	6.1	0.7–12.4	0.8–6.6	1.2–13.2	1.4–13.0	1.3–6.7	1.3–13.2	0.1–4.5	0.6	0.1–2.9	0.1–4.5	1.2	0.1–2.9	0.6–6.1	1.0–6.1
Suberinite	0.1–6.0	0.0–5.0	1.9	0.1–6.0	0.0–5.8	1.9	0.4–8.0	2.0–5.4	0.3–6.6	0.4–8.0	2.0–8.5	0.0–6.6	0.0–0.2	0.2	0.0–3.5	0.0–0.2	0.4	0.0–3.5	0.1–3.9	0.1–4.9
Exsudatinite	0.0–10.9	0.0–8.9	2.0	0.0–10.9	0.0–9.5	2.0	0.1–4.1	0.6–6.2	0.2–6.1	0.2–4.1	0.6–8.0	0.2–6.2	0.1–0.9	0.3	0.0–6.4	0.1–0.9	0.6	0.0–6.4	0.3–4.0	0.5–4.9
Liptinite group	0.3–18.4	7.0–41.5	21.8	0.3–18.4	7.0–44.4	21.8	7.5–34.2	6.8–34.2	10.2–36.6	7.5–35.98	6.8–34.7	10.2–37.0	0.3–12.2	2.0	0.8–20.5	0.3–12.2	4.0	0.8–20.5	2.0–25.3	4.0–26.3
Mineral matter	0.0–2.5	0.0–13.3	0.0	-	-	-	0.0–33.6	0.0–36.1	0.0–26.4	-	-	-	0.0	50.6	0.0–8.9	-	-	-	0.0–50.6	-
IV FACTOR	-	-	-	0.7–12.1	0.0–13.4	2.6	-	-	-	0.1–5.5	0.1–5.2	1.9–12.3	-	-	-	0.0–3.54	11.7	0.0–10.3	-	2.0–11.7
Coal facies Mukhopadhyay (1986)																				

Table 1 (continued)

Coal Section	MC 01						MC 12						MC 05						Avg	Avg
Seams	01/04	01/02–01/03	01/01	01/04	01/02–01/03	01/01	T	M	B	T	M	B	05/03	05/02	05/01	05/03	05/02	05/01		
A = hu (ht + hc) + terrestrial lp	-	-	-	72.7–95.1	79.7–99.3	89.8	-	-	-	69.9–94.4	83.1–97.8	83.7–92.5	-	-	-	68.0–99.8	86.9	73.9–99.5	-	83.9–90.0
B = hd + lp + pg	-	-	-	7.7–32.6	1.8–18.7	18.5	-	-	-	2.4–32.8	9.2–14.2	4.1–56.0	-	-	-	10.7–32.3	11.6	0.6–32.5	-	10.1–21.5
C = in	-	-	-	0.6–10.7	0.0–11.1	2.0	-	-	-	0.1–4.1	0.1–3.4	1.6–9.2	-	-	-	0.0–3.7	11.2	0.0–8.2	-	1.6–11.2
Singh and Singh (1996)																				
A = hu + lp	72.8–99.4	77.1–100	98.0	-	-	-	65.3–99.9	62.4–99.9	72.5–97.4	-	-	-	96.3–100	43.9	89.8–100	-	-	-	43.9–98.2	-
B = In	0.6–10.4	0.0–10.5	2.0	-	-	-	0.1–4.1	0.1–3.3	1.2–9.2	-	-	-	0.0–3.7	5.5	0.0–8.2	-	-	-	1.4–5.5	-
C = Mineral matter	0.0–2.5	0.0–13.3	0.0	-	-	-	0.0–33.6	0.0–36.1	0.0–26.4	-	-	-	0.0–0.0	50.6	0.0–8.9	-	-	-	0.0–50.6	-
Lamberson et al. (1991)																				
TPI	0.5–3.3	1.3–10.3	3.5	-	-	-	0.9–52.1	1.8–4.5	0.5–23.1	-	-	-	0.4–5.8	0.5	0.0–81.4	-	-	-	0.5–13.8	-
GI	7.8–23.6	0.0–133.4	37.4	-	-	-	17.7–902.0	19.0–953.0	8.4–52.3	-	-	-	0.0–17.2	7.7	0.0–1065	-	-	-	7.7–339.8	-
Calder et al (1991)																				
GWI	0.7–5.1	0.1–3.7	0.4	-	-	-	0.0–1.6	0.3–9.8	0.0–11.8	-	-	-	0.2–4.2	8.6	0.0–7.2	-	-	-	0.4–8.6	-
VI	3.5–220.9	1.7–233.0	3.4	-	-	-	0.7–45.4	0.4–43.2	0.6–19.0	-	-	-	7.9–87.5	15.4	0.6–228.6	-	-	-	3.4–55.7	-
Ash (wt. %, dry basis)	0.03–0.29	0.02–0.50	0.04–0.24	-	-	-	0.01–0.03	0.05–0.75	0.07–0.55	-	-	-	0.00–0.13	0.01–0.32	0.04–0.38	-	-	-	0.22	-

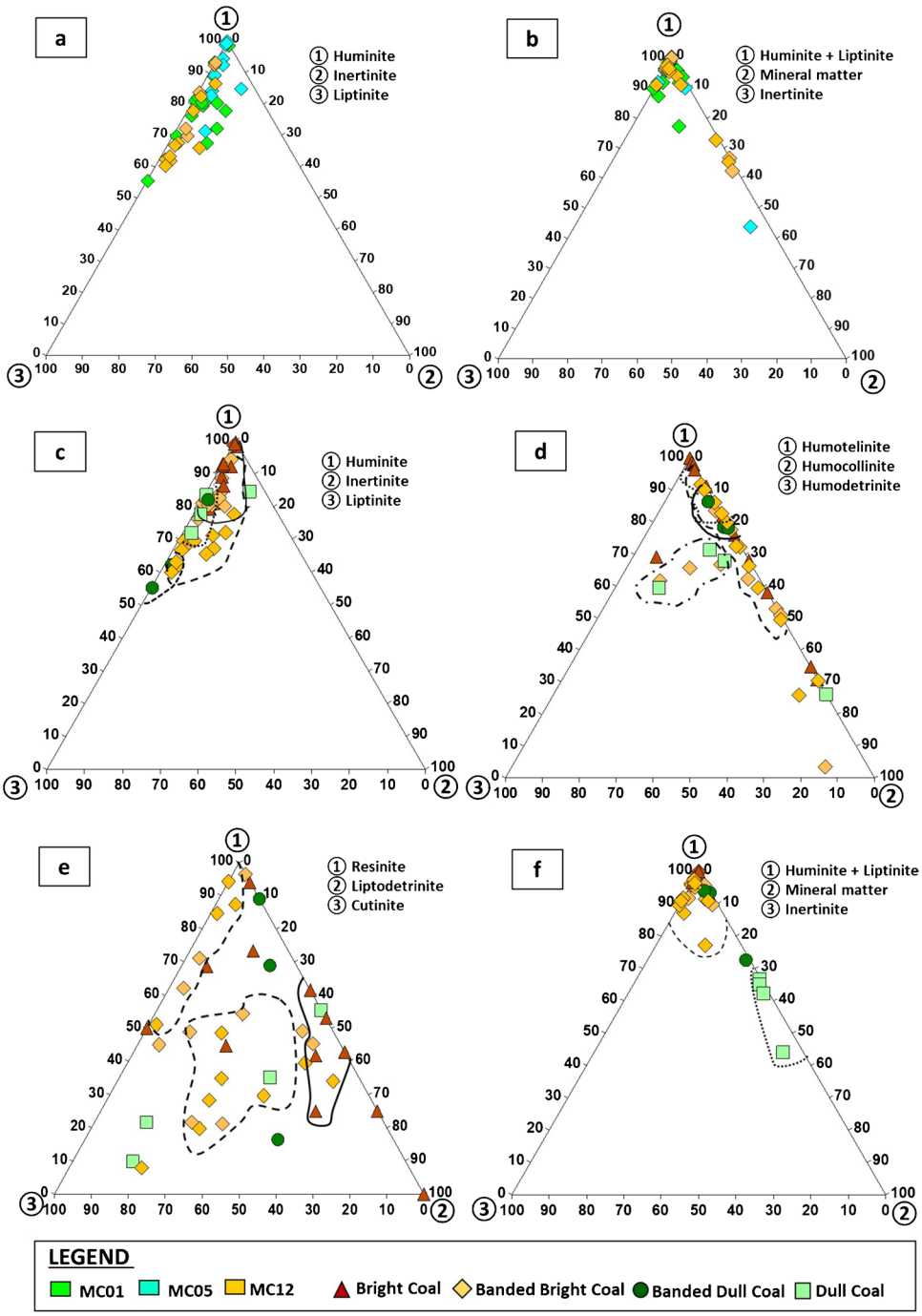

Fig. 4 Ternary diagrams show composition of (a) coal (vol.%, mmf); (b) coal (vol. %); (c) lithotypes (vol.%, mmf); (d) submacerals from the huminite group (vol.%, mmf); (e) relative proportions (vol%, mmf.) of resinite, cutinite, and liptodetrinite in the lithotypes; and (f) lithotypes (vol.%) for the studied Mukah coal in the Balingian Formation, Sarawak. The fields with the main coal lithotypes are shown in (c)–(f)

(74.5%–88.7% cmf). Humite was present as the most predominant monomaceral group and ranged from 5.5% to 61.1% (1.8%–12.5% cmf), with the highest concentration of humite was reported in seam MC05. Among trimaceral groups, duroclarite was the most common and occurred in low-to-moderate concentrations ranging from 0.0% to 8.5% (1.7%–18.7% cmf). The other microlithotypes, e.g., liptite, inertite, durite, huminertite, and huminertoliptite, in the coal constituted < 1% of most samples (Table 2). Carbominerite was reported in all samples, ranging from 0.0% to 67.9%, with the highest concentration reaching 67.9% in the dull lithotype (seam 05/02). The coal seams present in MC01 and MC05 showed an increase in carbominerite content toward the lower seams. In contrast, the seam in MC12 represents the enrichment of clastic minerals toward the seam top, indicating a high water increase toward the roof of the seam (Fig. 2, Table 2).

Table 2 Microlithotype compositions showing the range and average (avg.) values of the Mukah coal on a total (vol.%) and cmf basis (vol.%). The measured values for the coal facies analysis are also shown (Hacquebard and Donaldson 1969; Singh et al., 2010; Smyth 1984; Hunt 1982)

Coal Section	MC 01						MC 12						MC 05						Avg	Avg
Seams	01/04	01/02–03	01/01	01/04	01/02 -03	01/01	T	M	B	T	M	B	05/03	05/02	05/01	05/03	05/02	05/01		
	(vol. %)			(vol.%, cmf)			(vol. %)			(vol.%, cmf)			(vol. %)			(vol.%, cmf)			(vol. %)	(vol.%, cmf)
Humite	4.5–28.9	5.6–36.6	5.5	5.1–28.9	6.5–36.6	5.5	5.2–68.1	5.7–40.2	1.8–12.5	4.6–68.2	6.0–40.2	1.8–12.5	25.7–96.5	22.9	5.6–96.3	25.7–96.5	71.7	29.0–96.3	5.5–61.1	1.8–12.5
Liptite	0.0–0.6	0.0–3.9	0.0	0.0–0.6	0.0–4.4	0.0	0.0–1.5	0.0	0.0–3.8	0.0–1.7	0.0	0.0–4.3	0.0–0.3	0.6	0.0–3.9	0.0–0.3	1.9	0.0–0.5	0.0–0.8	0.0–4.3
Inertite	0.0–1.3	0.0–2.4	0.0	0.0–1.3	0.0–3.5	0.0	0.0–0.3	0.0–0.5	0.0–0.7	0.0–0.5	0.0–1.1	0.7–0.7	0.0–0.4	1.2	0.0–5.1	0.0–0.4	3.9	0.0–5.1	0.0–1.3	0.7–0.7
Clarite	55.6–88.1	39.5–86.3	88.7	55.6–88.1	57.1–89.7	88.7	19.4–80.8	37.7–80.8	50.3–88.2	31.7–86.2	59.7–84.7	74.5–88.7	3.3–63.5	3.5	3.4–76.4	3.3–63.5	10.9	3.4–63.0	3.5–88.7	74.5–88.7
Durite	0.0–7.5	0.0–6.7	0.0	0.0–8.4	0.0–6.7	0.0	0.0–0.2	0.0–0.2	0.1–1.4	0.0–0.2	0.0–0.4	0.1–1.4	0.0–0.7	3.1	0.0–3.6	0.0–0.7	9.6	0.0–0.8	0.0–3.1	0.1–1.4
Huminertite	0.0–1.6	0.0–1.1	0.1	0.0–1.6	0.0–1.3	0.1	0.0	0.0	0.0–0.1	0.0	0.0	0.0–0.1	0.2–1.3	0.7	0.0–3.0	0.2–1.3	1.9	0.0–3.0	0.0–0.9	0.0–0.1
Duroclarite	1.4–13.7	0.0–14.5	5.7	1.4–13.7	0.0–17.0	5.7	0.1–8.4	0.1–8.4	1.1–18.7	0.1–7.2	0.1–8.8	1.7–18.7	0.0–7.8	0.0	0.0–8.2	0.0–7.8	0.0	0.0–8.2	0.0–8.5	1.7–18.7
Clarodurite	0.0–0.5	0.0–0.3	0.0	0.0–0.6	0.0–0.3	0.0	0.0	0.0	0.0–0.2	0.0	0.0	0.1–0.2	0.0	0.0	0.0–0.1	0.0	0.0	0.0–0.1	0.0–0.1	0.1–0.2
Huminertoliptite	0.0–1.7	0.0–1.5	0.0	0.0–1.9	0.0–1.5	0.0	0.0	0.0	0.0–2.8	0.0–2.0	0.0	0.0–2.8	0.0–0.4	0.0	0.0–0.8	0.0–0.4	0.0	0.0–1.3	0.0–0.7	0.0–2.8
Carbominerite	0.0–11.0	0.0–37.5	0.0	-	-	-	0.1–74.6	0.0–4.8	0.0–43.2	-	-	-	0.0	67.9	0.0–14.5	-	-	-	0.0–67.9	-
Coal facies																				
Hacquebard & Donaldson (1969)																				
A = dc + hl	1.6–13.7	0.0–15.2	5.7	-	-	-	0.1–8.4	0.1–8.4	1.4–21.5	-	-	-	0.0–8.2	0.0	0.0–9.0	-	-	-	0.0–9.2	-
B = hi-I	0.0	0.0	0.0	-	-	-	0.0	0.0	0.0	-	-	-	0.0	0.0	0.0	-	-	-	0.0	-
C = cl + hu + hi-H	75.6–98.0	57.1–100	94.3	-	-	-	24.6–99.8	47.2–99.9	54.7–94.5	-	-	-	90.5–100	27.1	57.1–99.8	-	-	-	27.1–95.2	-
D = cd + du + cm	0.0–18.9	0.0–37.5	0.0	-	-	-	0.1–74.6	0.0–52.0	0.4–43.4	-	-	-	0.0–0.7	71.0	0.0–14.5	-	-	-	0.0–71.0	-
A + D	1.7–24.0	0.0–40.4	5.7	-	-	-	0.2–75.0	0.1–52.2	5.5–44.7	-	-	-	0.0–8.9	71.0	0.0–15.8	-	-	-	4.4–71.0	-
B + C	75.6–98.0	57.1–100	94.3	-	-	-	24.6–99.8	47.2–99.9	54.7–94.5	-	-	-	90.5–100	27.1	57.1–9.8	-	-	-	27.1–95.2	-
Singh et al. (2010)																				
hu + cl + lp + hu-H + dc + du-E + hl	79.6–99.9	62.5–100	99.9	-	-	-	25.4–99.9	47.5–100	56.6–99.5	-	-	-	97.7–99.8	27.0	62.5–99.9	-	-	-	27.0–99.9	-
in + hi-I + du-I + cl	0.1–9.4	0.0–8.9	0.1	-	-	-	0–0.5	0.0–0.7	0.1–2.2	-	-	-	0.2–2.3	5.0	0.0–8.3	-	-	-	0.0–5.0	-
Smyth (1984), Hunt (1982)																				
hu + cl	-	-	-	83.7–98.0	79.5–100	94.2	-	-	-	90.8–99.9	90.7–99.9	76.3–96.4	-	-	-	89.2–99.8	82.6	86.4–100	-	76.3–96.4
du + in	-	-	-	0.1–8.8	0.1–8.8	0.0	-	-	-	0.0–0.7	0.0–1.5	0.1–2.1	-	-	-	0.0–1.1	13.5	0.0–5.2	-	0.1–2.1
hi + dc + cd	-	-	-	1.5–15.2	0.0–18.3	5.8	-	-	-	0.1–7.2	0.1–8.8	1.7–18.8	-	-	-	0.2–9.0	1.9	0.0–10.9	-	1.7–18.8

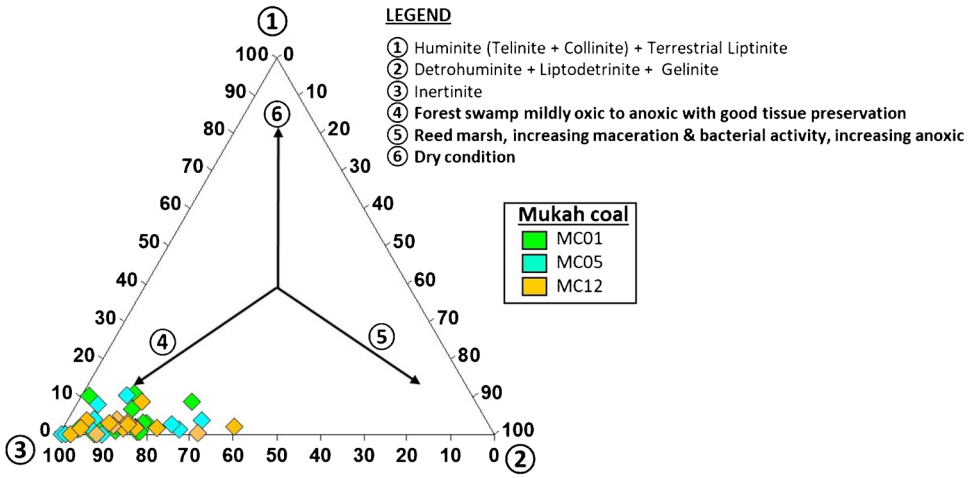

Fig.5 The coal facies modified after Mukhopadhyay (1986) showed a forest swamp under mildly oxic to anoxic peat development for the Mukah coal

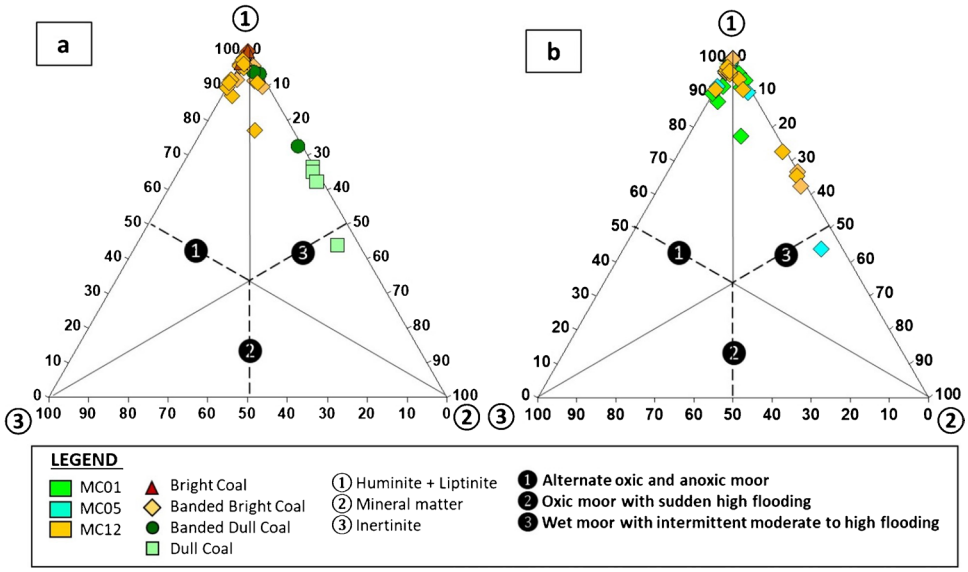

Fig. 6 The coal facies modified after Singh and Singh (1996) showed the depositional condition of (a) all lithotypes and (b) coal under oxic and anoxic conditions of a wet peatland for the Mukah coal

Ash contents

Ash yields of studied coal were < 1 wt. %, with an average range of 0.00–0.75 wt. % (Table 1). This was in good agreement with the low amount of mineral matter microscopically observed in all studied samples.

Discussion

Paleofacies and paleomires conditions

Six coal facies models proposed by Mukhopadhyay (1986), Singh and Singh (1996), Lamberson et al. (1991), Calder et al. (1991), Hacquebard and Donaldson (1969), and Singh et al. (2010) were developed and used to assess the paleofacies and paleomire conditions of the Neogene Mukah coal from the Balingian Formation, Sarawak. The concentrations, maceral indices, associations of the macerals, including the clastic mineral content and lithotype variations, were identified and analyzed for all studied samples (Table 1).

A facies-critical maceral association model modified after Mukhopadhyay (1986) was used to understand the deposition environment for the Late Miocene Mukah coal from the Balingian Formation. The results of the coal samples studied from the intra-seams indicated that the plots clustered and trended toward a forest swamp environment under mildly oxic to anoxic conditions, thus suggesting good tissue preservation (Diessel 1992) (Fig. 5).

Based on the facies diagram developed by Singh and Singh (1996) in Fig. 6a, for the coal facies, most of the brighter coal lithotypes plot at the edge of "1," related to a higher amount of huminite and lower amount of inertinite, thus indicating oxic moor facies. Moreover, the duller lithotypes with higher amounts of clay minerals indicated that these lithotypes primarily evolved under wet conditions with

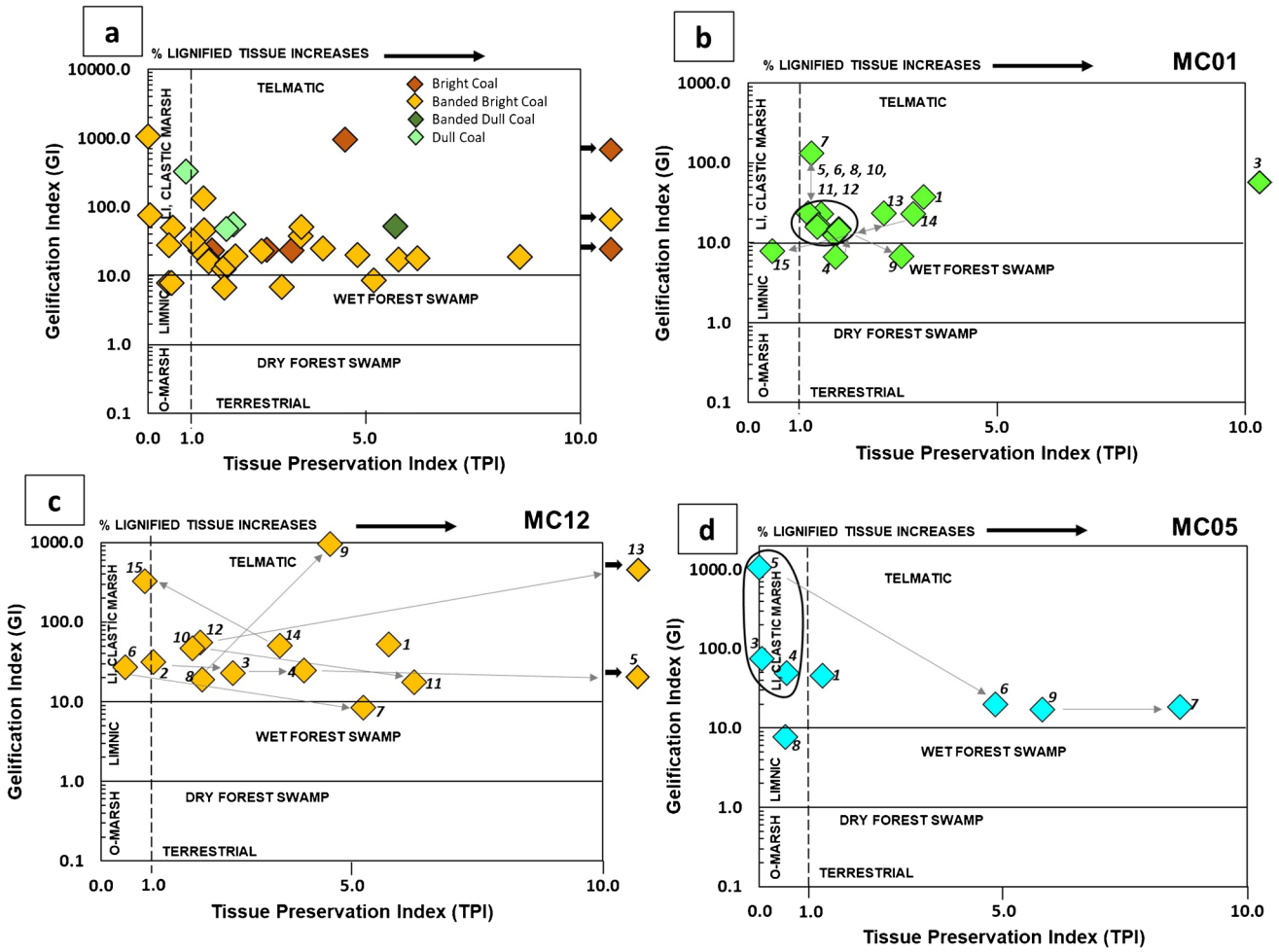

Fig. 7 Cross-plot of the GI and TPI based on in-seam variation samples (Lamberson et al. 1991) showing the depositional settings of (a) all lithotypes and sections (b) MC01, (c) MC12, and (d) MC05. The arrows indicate that the studied coal's depositional environment changed with time. The numbers indicate the phases of change in the paleomire, with the lowest number representing the bottom of the coal seam and the top marking the highest number

intermittent moderate to high flooding. Based on the plots of all studied samples (Fig. 6b), the peat formation evolved in wet, low-lying mires with intermittent moderate and high flooding. The plots were concentrated on the huminite + liptinite corner. However, there were a few samples from MC12 and one sample from MC05 that contained a moderate amount of mineral matter, explained by the intermittent moderate to high flooding that occurred during deposition at those sections. The expected tectonic instability in the wet conditions of the mires (e.g., Flores and Sykes 1996) was attributed to moderate to high water cover and intermittent to high flooding into the mires. The water table fluctuations in the basin were attributed to the steady subsidence rates of the raised mires, thus giving rise to moderate diversification of the macerals and a moderate amount of mineral matter.

The tissue preservation index (TPI) and gelification index (GI) indices developed by Diessel (1986) and later modified by Lamberson et al. (1991) were used to determine the coal facies by creating a connection between the facies' indicators and the coal formation environment. The formulae used are shown in Table 1. The lithotype plots on the facies diagram (Fig. 7a) demonstrated that the lithotypes mostly developed in telmatic zones, except for a few plots of the banded bright lithotype in the clastic marsh region. The lignified tissue increased in the brighter lithotype, resulting in the formation of huminite. The TPI versus GI plots of the in-seam variations (Fig. 7b–d) based on the average coal composition of the Mukah coal seams possessed high TPI-GI values; most samples had a high TPI (> 1), thus indicating that trees were present, and GI values of > 10, predominantly reflecting the topogenous conditions in the mire within the telmatic setting. The high productivity of the precursor of the peat, which was primarily humotelinite, was suggested to have been influenced by intermittent moderate-to-high flooded hydrologic conditions with minimum oxidation levels during the peat development. Moreover, the samples (e.g., seam

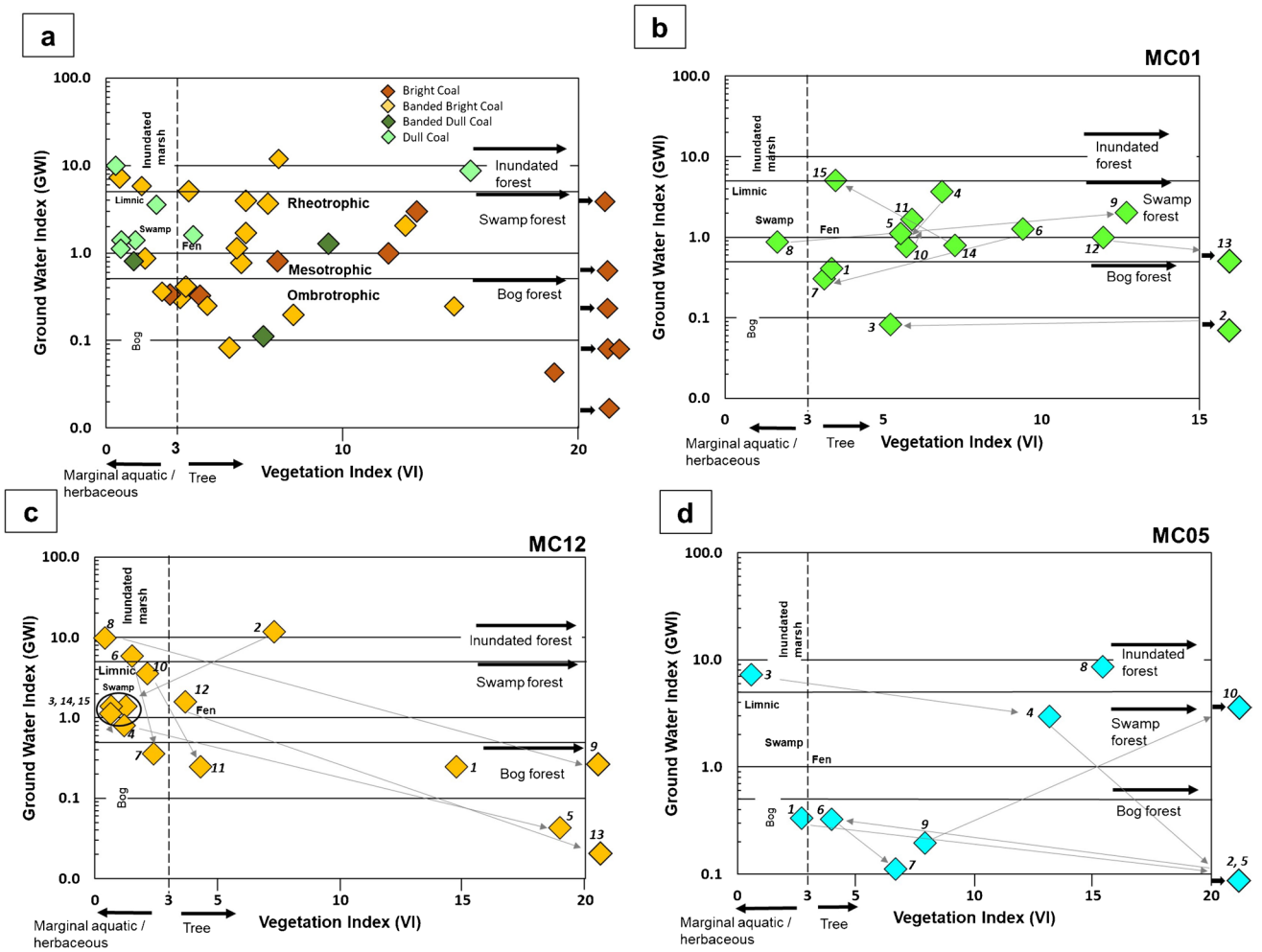

Fig. 8 Cross-plot of the GWI and VI indices based on in-seam variation samples (Calder et al. 1991) showing the depositional settings of (a) all lithotypes and sections (b) MC01, (c) MC12, and (d) MC05

05/02) that were rich in mineral matter indicated high flooding to the mire, with a high influx of clastic material during peat accumulation. Both conditions resulted in a lower liptinite content and minor inertinite content in the studied samples. Based on Diessel's (1986, 1992) work, the studied coal was exposed to mild humification and strong gelification of plant tissues because of the high rate of subsidence. Furthermore, the high TPI-GI values in the studied Mukah coal indicated that the mires originated from wet forest swamps (telmatic swamps) with a predominance of arboreal-rich vegetation (Lamberson et al. 1991). However, a few samples of the studied coal were characterized by a low TPI and high GI, suggesting the prevalence of herbaceous plants with enhanced humification in continuously wet raised bogs within a limno-telmatic regime (Diessel 1986, 1992).

The ground water index (GWI) and vegetation index (VI) indices proposed by Calder et al. (1991) explain the vegetation types from forest, herbaceous, and marginal affinities in the hydrogeological conditions of ombrotrophic, mesotrophic, and rheotrophic mires (Table 1). The lithotype variations on the coal facies diagram (Fig. 8a) demonstrated that the GWI and VI indices significantly varied for the bright and dull coals. Generally, the GWI values for the bright coals were lower than five, indicating rheotrophic to (mostly) ombrotrophic conditions. However, the duller coal lithotype showed moderate-to-high GWI values (> 1), which suggested (mostly) rheotrophic to inundated hydrologic regimes. Nevertheless, the banded lithotypes were situated in the ombrotrophic to inundated hydrological regions on the plot. In general, all lithotypes were formed under low-to-moderate water floods maintained by rainfall and the groundwater level. In this study, many of the banded bright and dull lithotypes of the Mukah coal appeared to have been formed under the influence of a moderate influx of siliciclastic deposits during peat accumulation because a high mineral content was reported in those samples (Calder et al. 1991). Variations in the GWI and VI indices of all studied coal (Fig. 8b–d) indicated most of the coal was

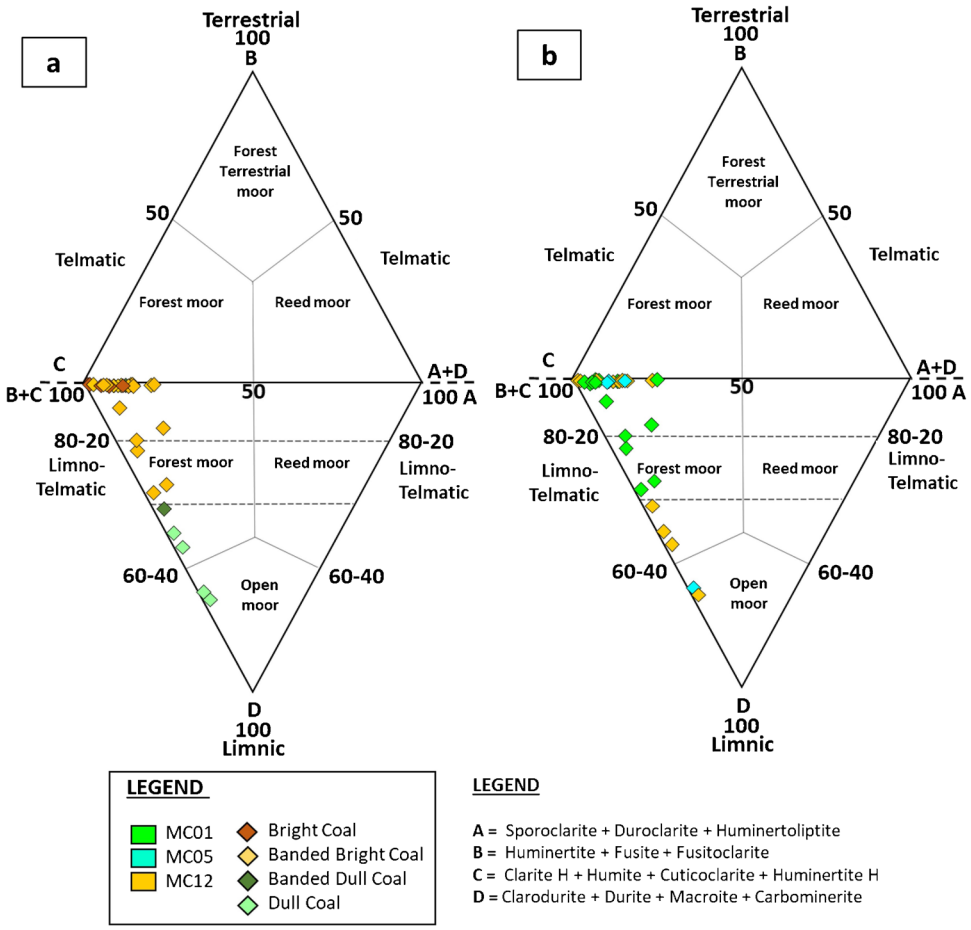

Fig. 9 Triangular diagram of coal facies modified after Hacquebard and Donaldson (1969) showing the (a) depositional condition of the brighter lithotypes, mainly under the forest moor, with the duller lithotypes having developed in a (mainly) limno-telmatic to open moor environment. (b) The depositional condition of the Mukah coal was mainly in telmatic forest moor zones

possibly deposited in a mire characterized by rheotrophic to ombrotrophic hydrologic regimes. In these conditions, the nutrient supply for the coal development in the mire was maintained by both groundwater and rainfall. However, certain plots were situated in the GWI sector over five, indicating a waterlogged environment within an inundated marsh to inundated forest (Fig. 8c–d). This condition may be related to inundations characterized by a higher influx of minerals. The results on the average composition of the coal seams demonstrated that most plots were concentrated on GWI values below three, thus suggesting a general predominance of telmatic conditions during the peat deposition at the Balingian Formation (Calder et al. 1991). In this case, most of the coal had a high VI (> 3), indicating that there was a prevalence of structured tree-derived material as the precursor vegetation in the mire and that the survival of vegetal tissues occurred under comparatively higher pH and lower Eh levels. However, some of the coal was dominated by herbaceous plants (VI < 3). Both GWI and VI values of the coals from the topmost section (MC01) of the Mukah coal suggest the deposition of peat, primarily in a swamp forest. In contrast, the middle (MC12) and lower section coals (MC05) are indicative of the bog forest paleoenvironment.

The plots in the facies model proposed by Hacquebard and Donaldson (1969), based on the microlithotype analyses (Fig. 9a), show that those of the bright and banded bright coal lithotypes mostly fell under the telmatic forest moor region, with a few lying in the limno-telmatic forest moor environment. This indicates relatively wet conditions during peat formation. Under these conditions, the survival of vegetal tissues occurred under comparatively higher pH and lower Eh levels. However, in the facies diagram, the duller coal demonstrated a distribution from the open moor (limnic) to (mainly) limno-telmatic forest moor region. The limnic region suggested a subaquatic environment in which the increase of circulation and energy levels was attributed to the peat formation. Based on the in-seam variations (Fig. 9b), most of the coal in MC01 was suggested to have originated in a telmatic coal facies during the formation of the precursor peats. However, the facies model for the precursor peat of MC05 and MC12 indicated a formation from limno-telmatic to telmatic coal facies (mostly). The lower stratal section of MC05 was characterized by a change from a limno-telmatic coal facies at the base to a telmatic coal facies at the top. However, a subaquatic coal facies occurred in the middle part of the section. The middle stratal section

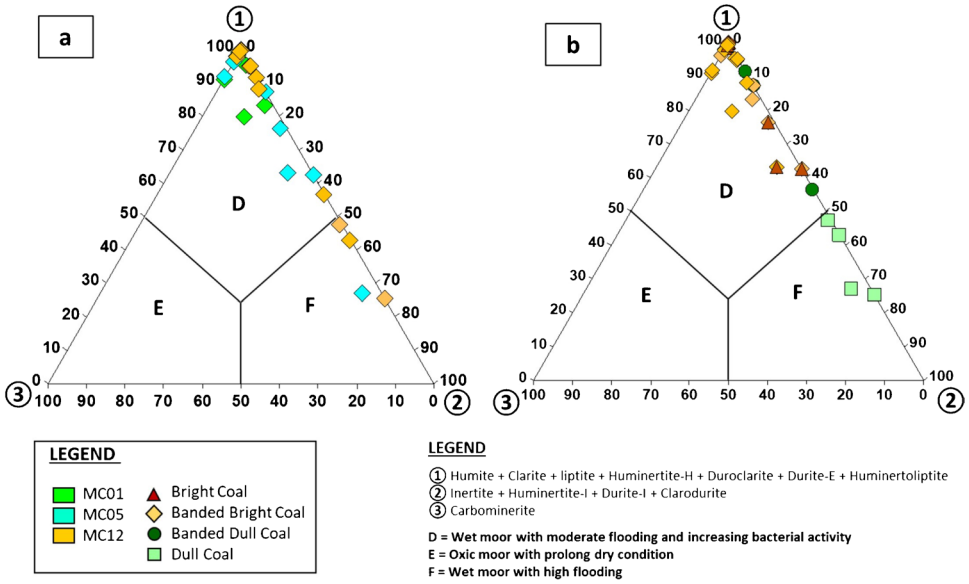

Fig. 10 Triangular diagram of the coal facies modified after Singh et al. (2010) showing the depositional condition of (a) all lithotypes and (b) the coal in mostly wet moor conditions for the Mukah coal

at MC12 demonstrated a trend from telmatic coal facies at the base to limno-telmatic facies toward the middle and telmatic coal facies at the top.

The lithotype plots of the coal facies diagram by Singh et al. (2010) demonstrated a significant contrast between dull coal and other lithotypes (Fig. 10a). The dull lithotypes primarily evolved under high flooding events, while the other lithotypes predominated a facies moor related to moderate flooding events with increased bacterial activity. Moreover, the duller lithotypes demonstrated an increase in carbominerite attributed to the fluctuations of the water level during peat accumulation. The plots of the in-seams samples favored the Mukah coal development to have occurred in a wet moor environment (Fig. 10b). The coal seams in the upper section (MC01) were formed and exposed to moderate flooding, thus resulting in less diversification in the microlithotypes. Furthermore, the coal seams in the middle and lower sections of the coal-bearing strata (MC05 and MC12, respectively) were developed during moderate to high flooding of water influx into the environment, thus resulting in a low to high percentage of carbominerite concentration. This resulted in the varying concentrations of preserved anaerobic organic matter in the coal.

Peat development and paleomire trends

The vertical variations in the lithotype and maceral composition (Fig. 11) and changes in the coal facies (Figs. 7b–d, 8b–d) reflect changes in the original peat mire environment for the Mukah coal. Compared with modern tropical peats (e.g., Amijaya and Littke 2005), a model for the growth of a domed paleo-peat (from the bottom to top sections) in the Mukah coal could be identified; however, the pattern was sometimes incomplete. In the Mukah coal, the occurrence of a complete succession from topogenous to ombrogrenous peat evolution is identified in the top portion of the lower stratal section (MC05, 122.5–123.5 m, Fig. 11). The middle (MC12) and topmost (MC01) sections of the Mukah coal comprised more than one succession of peat development, mostly incomplete ombrogenous peat development. In certain intra-seams, the top part of the seam was developed in the topogenous peat although it began with ombrogenous peat development in the paleomire. This reverse order of paleo-peat bodies has been reported by Sia et al. (2014). While most seams demonstrated changes in peat development, certain intra-seams had developed in either topogenous or ombrogenous peat only, in particular at 114.5–115.5 m and 46–47 m intervals (Fig. 11). From planar to domed peat, the peat's doming was represented by the predominance of humocollinite-liptinite-rich coal or humocollinite-mineral matter rich coal in the lower stratal section; however, the middle section was characterized by humotelinite-rich and finally overlain by humotelinite-liptinite rich coal in the topmost section (Fig. 11).

The basal section of each complete/incomplete paleo-peat trend containing a high concentration of liptinite was originally reported by Dehmer (1993) and Mukhopadhyay (1991, unpublished data cited in Esterle and Ferm 1994) and indicated that sapric peat or fine hemic peat may have developed under subaquatic conditions. As per Teichmüller (1989), under these conditions, liptodetrinite is abundant, as was observed in our studied coal. In this study, humodetrinite was observed to commonly occur at the base of the intra-seams, indicating the sapric peat accumulated in the limno-telmatic setting. In several cases, the basal section of the coal benches was moderate to high in detrital/mineral matter (Fig. 11), representing the high carbominerite in most of these samples (Fig. 11) and suggesting that the

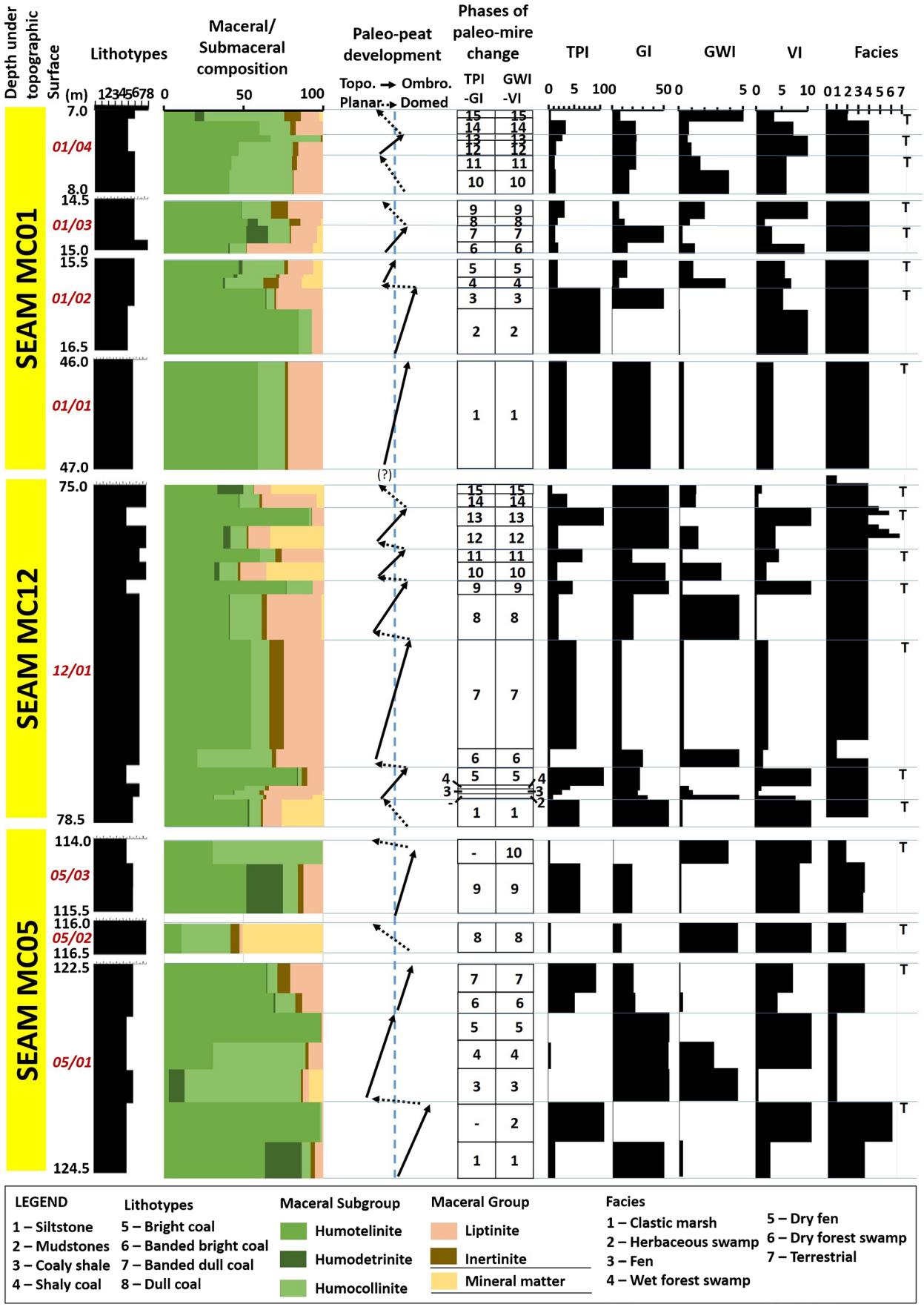
Depth under topographic Surface
Lithotypes
Maceral/ Submaceral composition
Paleo-peat development
Topo. → Ombro.
Planar → Domed
Phases of paleo-mire change
TPI -GI
GWI -VI
TPI
GI
GWI
VI
Facies
SEAM MC01
SEAM MC12
SEAM MC05
01/04
01/03
01/02
01/01
12/01
05/03
05/02
05/01
LEGEND
Lithotypes
1 – Siltstone
2 – Mudstones
3 – Coaly shale
4 – Shaly coal
5 – Bright coal
6 – Banded bright coal
7 – Banded dull coal
8 – Dull coal
Maceral Subgroup
Humotelinite
Humodetrinite
Humocollinite
Maceral Group
Liptinite
Inertinite
Mineral matter
Facies
1 – Clastic marsh
2 – Herbaceous swamp
3 – Fen
4 – Wet forest swamp
5 – Dry fen
6 – Dry forest swamp
7 – Terrestrial

◂**Fig. 11** Paleo-peat development. Also shown are the maceral group/subgroup compositions and mineral matter of the analyzed Mukah coal. Note that the numbers of paleomires are shown in Figs. 7–8 and that T is the top section of the peat body/coal bench

influx in river deposits occurred during a rise of the water table into the mires. As per Littke and Lo (1989) and Grady et al. (1993), a high content of mineral matter is indicated by a continuous evolution from seat earth to coal, which was reported in the studies on modern tropical peats by Dehmer (1993), Neuzil et al. (1993), and Esterle and Ferm (1994), who reported ash-rich layers. However, the studied coal generally had a poor ash yield (average 0.22 wt. %). As per Esterle and Ferm (1994), lack of identification of high-ash coal at the base section of a sequence could indicate the following: (1) a total absence; (2) layers too thin to be recognized; (3) a reduction in thickness because of overburden compaction; or (4) its inclusion in the seat earth because of a high ash content and gradational nature.

The middle section of the paleo-peat trend in the humotelinite-rich Mukah coal was believed to be the precursor of the hemic and fine hemic peats (Fig. 11). Previous researchers reported that these peats are characterized by wood fragments, logs, and stumps (Esterle et al. 1989; Dehmer 1993; Supardi et al. 1993 and Esterle and Ferm 1994), with the compacted humic attritus as the matrix (Anderson 1983; Esterle and Ferm 1994). As per other reports on modern tropical domed peats (e.g., Dehmer 1993; Grady et al. 1993; Esterle and Ferm 1994; Amijaya and Littke 2005), the enrichment of textinite in hemic peat is often associated with structured huminite with some cell fillings (corpohuminite). In this study, phlobaphinite and porigelinite were reported to be the common macerals in this section, indicating plant communities rich in wood (Cohen 1968; Taylor et al. 1998). Thus, the precursors of peat for the middle section of the studied paleo-peat bodies could be interpreted as having been dominated by wood-producing plants and originally deposited in a swamp rich in wood-producing trees. The increase of humotelinite in the middle section was associated with the decrease in the humocollinite and humodetrinite, furthermore supports the increasing mires of forest types under relatively dry conditions (Sia et al., 2012b).

The top section of the studied paleo-peat bodies was represented by humotelinite-liptinite-rich coal (> 70%). This section was believed to reflect the fibric peat of the modern peat in this area (Fig. 11). In other modern peat studies, fibric peat is rich in humodetrinite (e.g., Grady et al. 1993; Amijaya and Littke 2005) as well as inertinite, primarily fusinite (e.g., Demchuk and Moore 1993; Dehmer 1993). They are a result of decreasing nutrient levels, thus affecting the plant size and arborescence (Esterle and Ferm 1994), as well as an increase in oxidized plant material through a fungal mechanism in response to an abnormally fluctuating water table close to the top of the peat (Dehmer 1993; Moore et al. 1996). In this study, however, the fibric peat was characterized by textinite- and/or ulminite-rich macerals in most of the studied coal. This section was primarily represented by bright and occasional bright banded coal with inertinite reported in various amounts (mostly < 10%). According to Esterle et al. (1989), based on studies of a domed peat deposit in Sarawak, the fibrous peats in the upper central portion of the deposit contained more preserved plant material than the peats toward the base and margins, which, although more degraded, contained large wood fragments (5–150 cm). Moreover, the deposit produced bright coal seams with bright vitrain bands of variable thicknesses (Esterle et al. 1989). These results were consistent with the results of this study, wherein the vegetation index was observed to increase toward the fibrous peat in the top section of the studied coal (Fig. 11).

As per Shearer et al. (1994) and Greb et al. (2002), most Cenozoic coal is composed of multiple stacked paleo-peat bodies. In this study, accumulations of different paleomires representing the paleo-peat environment were recognized because of the occurrence of inorganic partings and organic, non-oxidized degradative partings. Recognizable bands of mineral-rich and/or humodetrinite-rich paleo-peat typical of topogenous deposits were developed in the sapric, hemic, or fine hemic peat of the Mukah coal (Fig. 11). The oxidized organic partings, however, were not used as an indicator of stacked paleo-peat bodies because of the less common inertinite-rich coal. This suggested that the ombrogenous peats in the Mukah coal were mostly free of clastic partings and low in ash yields and pyrite. Similar scenarios have been reported in studies of other ombrogenous peats in modern tropical climates (Esterle and Ferm 1994; Greb et al. 2002; Amijaya and Littke 2005; Davis et al., 2007; Súarez-Ruiz et al. 2012; O'Keefe et al. 2013). The most probable explanation for this condition was the peat doming where the rainfall was higher than the evaporation (Cohen et al. 1987) and limited suspension of sediment influx from the river (Amijaya and Littke 2005). Because the growth of pyrites is dependent on the sulfur content, raised bogs have a low sulfur content (Cameron et al. 1989; Neuzil et al. 1993). Thus, the domed peat development of the Mukah coal was probably attributed to an acidic, mildly oxidizing environment that resulted in conditions unfavorable for pyrite formation (Amijaya and Littke 2005) or inertinite. Furthermore, for the topogenous peat, the occurrence of pyrites in the studied coal was uncommon, suggesting that the peat accumulation occurred in freshwater mires with little or no marine influence. During the peat accumulation, the freshwater mires were subjected to periodic inundations by the fluvial input into the mire during a rising water table.

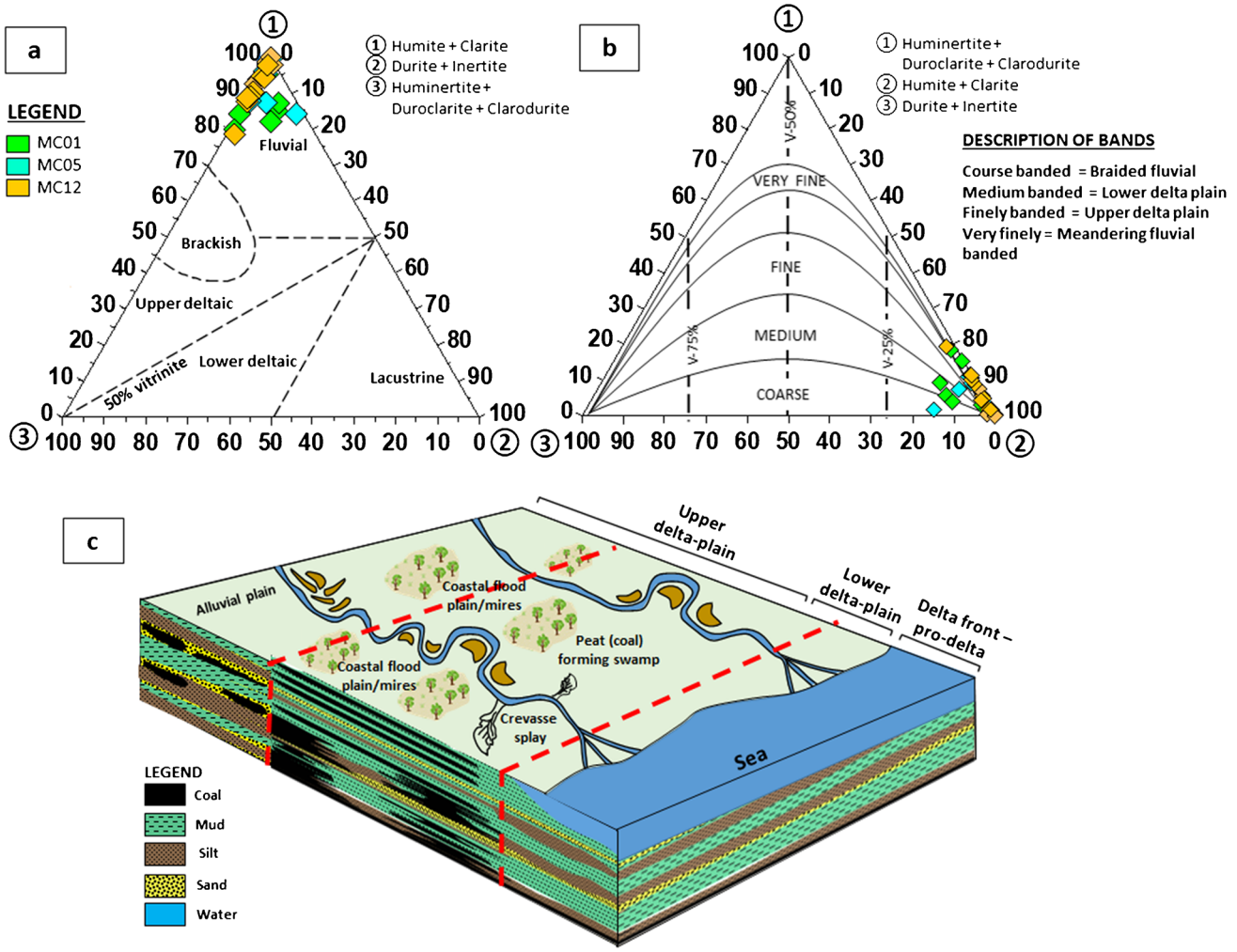

Fig. 12 Triangular diagrams based on microlithotypes (cmf) after (a) Smyth (1984) and (b) Hunt (1982) illustrating that the coal depositional environment for the Mukah coal was a predominantly fluvial–deltaic setting mainly the upper delta plain

Regarding the lithotypes, the changes from topogenous to ombrogenous peat were characterized by an increase in the brightness of the coal lithotypes. In this study, the ombrogenous peat was primarily characterized by bright and banded bright lithotypes, while topogenous peat was predominantly characterized by banded dull and dull lithotypes. The transition (mesotrophic) peat had variable coal lithotypes. Thus, a dulling-up sequence that developed toward the ombrogenous peat, as seen in many Paleozoic and Mesozoic coals, was absent in this study, as inertinite was uncommon at the top part of the dome. The same scenario was discussed in detail by Esterle et al. (1989) and Moore and Ferm (1992).

Paleodepositional environment of coal

Two depositional models based on the microlithotype groups were used to distinguish between the coal from different depositional environments. The depositional model developed by Smyth (1984) based on the density of microlithotype groups (free of carbominerite) in Fig. 12a suggested that the Mukah coal was predominantly fluvial in origin, as all plots were concentrated at edge "1," high in humite and clarite. Hunt (1982) proposed a ternary diagram by adding a fourth bandwidth, which demonstrated that the Mukah coal primarily originated in meandering fluvial deposits in the lower to upper coastal plain (Fig. 12b), as most coal lithotypes preserved very fine coal bands. Several plots, however, occurred in a fine- to medium-banded region, indicating a depositional environment in the upper to lower delta plain. The former prevailed most of the time, while the latter occurred in certain stages of the peat development. Section 3.1 shows that models that were supported by the megascopic assessment of the coal-bearing succession.

In comparison, Sia et al.'s (2014) study reported a predominance of marsh fields in a limno-telmatic environment of the lower delta plain, whereas most samples in this study

primarily originated in a swamp–bog forest moor of (mainly) telmatic to limno-telmatic coal facies in the fluvial–deltaic environment (Fig. 12c). The current interpretation was supported by the Southeast Asia peatland studies described by Anderson (1964, 1983), who reported that the interior portions of the extensive lowland forest bogs in Sumatra, Borneo, and the Malay Peninsula are ombrotrophic but that their seaward spreading behind the coastline is primarily a topogenic occurrence. In this study, the raised peat surfaces confine the river and tidal floods to their respective channels, thus resulting in the majority being only slightly flooded and thus relatively clean with low inertinite and ash content of typically < 2% (Anderson 1964, 1983). Mostly, arborescent plant types were predominant. The wet mires' deposition environment was consistent with the low IV factor reported for all samples, interpreted by Diessel (1992) as a wet forested deposit. The slight modification in the interpretation of the deposition environment from the previous studies by Sia et al. (2011, 2014) and Hakimi et al. (2013) could possibly be explained by where the studied coal sections developed further inland (Fig. 1b), toward the coastal floodplain area in the upper delta plain setting, in which telmatic coal facies are more prominent in the mires (Fig. 12c).

The depth of the water and water table fluctuations affected both the different vegetation ecosystems and deposition of the peat mires and governed the way the petrographic entities were preserved (Bohacs and Suter 1997; Diessel 2007; Herbert 1997; Holz et al. 2002; Singh and Shukla 2004). In this study, the coal facies models used had confirmed the events of water level fluctuation during the peat development in the basin and the coal primarily developed in a continuously wet swamp forest to a raised forested bog with a predominance of trees in the peatland. Furthermore, terrestrial, fen, dry fen, dry forest, and swamp facies appeared to be unusual and consistently supported by the ever-wet climate that was favorable during the development of the Neogene coal of the Balingian Province of the Sarawak Basin (Sia et al 2014).

Conclusion

The following conclusions could be obtained:

1. In this study, a high huminite and moderate liptinite content typified the coal while inertinite and mineral matter were uncommon. Little to no alginite and pyrite was observed. Clarite predominated throughout the studied coal. The lithotype brightness increased as the huminite content increased, while the lithotype dullness was primarily attributed to the presence of liptinite and mineral matter. Similarly, an increase of humite and decrease in clarite, duroclarite, and carbominerite occurred in the brighter lithotypes (bright and banded bright).
2. The facies modeling analysis using the maceral composition, indices, and associations suggested that the coal and brighter lithotypes primarily developed in a continuously wet swamp forest to a raised forested bog with mixed paleodepositional conditions from mildly oxic to anoxic conditions within telmatic forest moor zones. The duller lithotypes evolved in limno-telmatic zones under increase in flooding.
3. Bright and banded bright lithotypes primarily characterized the ombrogenous peat, while banded dull and dull lithotypes predominated in the topogenous peat. A complete succession from topogenous to ombrogrenous peat in the telmatic to limno-telmatic environment was mostly reported in the paleo-peat bodies. The peat doming was represented by a predominance of humodetrinite/liptinite-rich coal or humocollinite/mineral matter-rich coal in the bottom section; however, the middle section was characterized by humotelinite- and humocollinite/liptinite-rich coal, which was overlain by humotelinite-rich coal in the top section. The source of the coal was suggested to have been primarily derived from arborous vegetation with a predominance of trees in the peatland.
4. A coastal floodplain setting within the (primarily) upper to lower delta plain environment was suggested for the evolution of the Mukah coal.

Acknowledgements The authors are very thankful to the Sarawak Coal Resource coal mining company in the Balingian coalfield, Sarawak, for providing borehole samples. The first author is most fortunate for financial assistance from the research grant YUTP-FRG (Cost Center 0153AA-E82) from Universiti Teknologi PETRONAS. Financial help from the University of Malaya research grant IPPP, PG315-2016A is appreciated.

Declarations

Funding and/or Conflicts of interests/Competing interests The authors declare that they have no known competing financial interests or personal relationships that could have appeared to influence the work reported in this paper.

Statements and declarations We, the undersigned, hereby declare that this manuscript is original, has never been published before, and is not currently being considered for publication elsewhere.

We confirm that all named authors read and approved the manuscript and that there are no other individuals who satisfied the criteria for authorship but are not listed. We also confirm that the authorship order listed in the manuscript has been approved by all of us.
We understand that the Corresponding Author is the sole contact during the Editorial process. He is responsible for communicating with the other authors about progress, submissions of revisions, and final approval of proofs.

References

Abdullah Wan Hasiah (1997a) Common Iiptinitic constituents of Tertiary coals from the Bintulu and Merit-Pila coalfield, Sarawak and their relation to oil generation from coal. Bulletin of the Geological Society of Malaysia 41:85–94. https://doi.org/10.7186/bgsm41199708

Abdullah WH (1997b) Evidence of early generation of liquid hydrocarbon from suberinite as visible under the microscope. Org Geochem 27 (7-8): 591–596. https://doi.org/10.1016/S0146-6380(97)00085-5

Abdullah WH (2002). Organic petrological characteristics of limnic and paralic coals of Sarawak. Bull Geo Soc Malays 45: 65–69.

Amijaya H, Littke R (2005) Microfacies and depositional environment of Tertiary Tanjung Enim low rank coal, South Sumatra Basin, Indonesia. Int J Coal Geol 61:197–221. https://doi.org/10.1016/j.coal.2004.07.004

Anderson JAR (1964) The structure and development of the peat swamps of Sarawak and Brunei. J Trop Geo 18:7–16

Anderson JAR (1983) The tropical peat swamps of western Malesia. In: Gore AJP (ed) Ecosystems of the World 4B, Mires: Swamp, Bog, Fen and Moor. Elsevier, Amsterdam, pp 181–198

Anon (1981) Coal interpretation manual. BPB Instruments Limited, East Leake.

ASTM D5142 (2009) Standard Test Methods for Proximate Analysis of the Analysis Sample of Coal and Coke by Instrumental Procedures. ASTM International, West Conshohocken. https://doi.org/10.1520/D5142-09

Bohacs K, Suter J (1997) Sequence stratigraphic distribution of coaly rocks: fundamental controls and paralic examples. AAPG Bull 81:1612–1639. https://doi.org/10.1306/3B05C3FC-172A-11D7-8645000102C1865D

Calder JH, Gibling MR, Mukhopadhay K (1991) Peat formation in a Westphal B piedmont setting, Cumberland Basin, Nova Scotia: Implications for the maceral-based interpretation of rheotrophic and raised paleomires. Bull Soc Geol Fr 162:283–298

Cameron CC, Esterle JS, Palmer CA (1989) The geology, botany and chemistry of selected peat-forming environments from temperate and tropical latitudes. Int J Coal Geol 12:105–156. https://doi.org/10.1016/0166-51628990049-9

Chen SP (1986) Coal potential and exploration in Sarawak. Bull Geol Soc Malays 2:649–665

Cohen AD, Spackman W, Raymond R (1987) Interpreting the characteristics of coal seams from chemical, physical, and petrographic studies of peat deposits. In: Scott AC (ed) Coal and coal-bearing strata: recent advances. Geol Soc Spec Publ 32: 107–125. https://doi.org/10.1144/GSL.SP.1987.032.01.08

Cohen AD (1968) The petrology of some peats of southern Florida with special reference to the origin of coal. PhD Dissertation, Pennsylvania State University, USA, pp. 352.

De Silva S (1986) Stratigraphy of south Mukah-Balingian region. Sarawak News GSM 12:215–219

Dehmer J (1993) Petrology and organic geochemistry of peat samples from a raised bog in Kalimantan Borneo. Org Geochem 20:349–362. https://doi.org/10.1016/0146-63809390125-U

Demchuk T, Moore TA (1993) Palynofloral and organic characteristics of a Miocene bog-forest, Kalimantan, Indonesia. Org Geochem 20:119–134. https://doi.org/10.1016/0146-63809390032-7

Diessel CFK (1986) On the correlation between coal facies and depositional environment. 20th Newcastle Symposium: Advances in the Study of the Sydney Basin. April 3rd-5th 1986, Newcastle, Australia, pp. 19–22.

Diessel CFK (1965) Correlation of macro- and micropetrography of some New South Wales coals. 8th Commonwealth Mining and Metallurgical Congress Melbourne 1965. Proceeding 6:669–677

Diessel C (1992) Coal-bearing Depositional Systems: Berlin, Springer-Verlag, 721 p.

Diessel C (2007) Utility of coal petrology for sequence-stratigraphic analysis. Int J Coal Geol 70:3–34. https://doi.org/10.1016/j.coal.2006.01.008

Esterle JS, Ferm JC, Tie YL (1989) A test for the analogy of tropical domed peat deposits to "dulling up" sequences in coal beds-preliminary results. Org Geochem 14:333–342. https://doi.org/10.1016/0146-63808990060-0

Esterle JS, Ferm JC (1994) Spatial variability in modern tropical peat deposits from Sarawak, Malaysia and Sumatra, Indonesia: analogues for coal. Int J Coal Geol 26:1–41. https://doi.org/10.1016/0166-51629490030-2

Flores RM, Sykes R (1996) Depositional controls on coal distribution and quality in the Eocene Burnner Coal Measures, Buller Coalfield, South Island, New Zealand. Int J Coal Geol 29:291–336. https://doi.org/10.1016/0166-51629500028-3

Grady WC, Eble CF, Neuzil SG (1993) Brown coal maceral distributions in a modern domed tropical Indonesian peat and a comparison with maceral distribution in Middle Pennsylvanian age Appalacian bituminous coal beds. In: Cobb JC Cecil CB (ed) Modern and ancient coal-forming environment. Geol Soc Am Spec Pap 286: 63–82. https://doi.org/10.1130/SPE286-p63

Greb SF, Eble CF, Hower JC, Andrews WM (2002) Multiple-bench architecture and interpretations of original mire phases - examples from the Middle Pennsylvanian of the Central Appalachian Basin, USA. Int J Coal Geol 49:147–175. https://doi.org/10.1016/S0166-51620100075-1

Hacquebard PA, Donaldson JR (1969) Carboniferous coal deposition associated with flood-plain and limnic environments in Nova Scotia. In: Dapples EC Hopkins ME (ed) Environments of Coal Deposition. Geol Soc Am Spec Pap 114: 143–191. https://doi.org/10.1130/SPE114-p143

Hakimi MH, Abdullah WH, Sia SG, Yousif MM (2013) Organic geochemical and petrographic characteristics of Tertiary coals in the northwest Sarawak, Malaysia: Implications for palaeoenvironmental conditions and hydrocarbon generation potential. Mar Pet Geol 48:31–46. https://doi.org/10.1016/j.marpetgeo.2013.07.009

Hennig-Breitfeld J, Breitfeld HT, Hall R, BouDagher-Fadel M, Thirlwall M (2019) A new upper Paleogene to Neogene stratigraphy for Sarawak and Labuan in northwestern Borneo: Paleogeography of the eastern Sundaland margin. Earth Sci Rev 190:1–32. https://doi.org/10.1016/j.earscirev.2018.12.006

Herbert C (1997) Relative sea-level control of deposition in the Late Permian Newcastle Coal Measures of the Sydney basin. Australia Sediment Geol 107:147–166. https://doi.org/10.1016/S0037-07389600027-9

Holz M, Kalkreuth W, Banerjee I (2002) Sequence stratigraphy of paralic coal-bearing strata: An overview. Int J Coal Geol 48:147–179. https://doi.org/10.1016/S0166-51620100056-8

Hower JC, Wagner NJ (2012) Notes on the methods of the combined maceral/microlithotype determination in coal. Int J Coal Geol 95:47–53. https://doi.org/10.1016/j.coal.2012.02.011

Hunt JW (1982) Relationship between microlithotype and maceral compositions of coals and geological setting of coal measures in the Permian basins of eastern Australia. Aust Coal Geol 4:484–502

Hutchison CS (2005) Geology of North-west Borneo: Sarawak, Brunei and Sabah. First (ed), Elsevier, New York, USA.

International Committee for Coal and Organic Petrography (ICCP) (1998) The new vitrinite classification ICCP System 1994. Fuel 77:349–358. https://doi.org/10.1016/S0016-23619880024-0

International Committee for Coal and Organic Petrology (ICCP) (2001) The new inertinite classification ICCP System 1994. Fuel 80:459–471. https://doi.org/10.1016/S0016-23610000102-2

Irwan I, Nair P, Tunio SQ (2012) Forecasting CBM Production of Mukah-Balingian Coalfield, Sarawak, Malaysia. Res J Appl Sci Eng Technol 4(21):4265–4274

Lamberson MN, Bustin RM, Kalkreuth W (1991) Lithotype maceral composition and variation as correlated with paleowetland environments, Gates Formation, Northeastern British Columbia, Canada. Int J Coal Geol 18:87–124. https://doi.org/10.1016/0166-51629190045-K

Liechti P, Roe FW, Haile NS (1960) The Geology of Sarawak, Brunei and the Western Part of North Borneo, 360 p

Littke RH, Ten Haven Lo (1989) Palaoecologic trends and petroleum potential of Upper Carboniferous coal seams of western Germany as revealed by their petrographic and organic geochemical characteristics. Int J Coal Geol 13: 529–574. https://doi.org/10.1016/0166-51628990106-7

Mazlan M (1999) Geological setting of Sarawak. In: Mansor MI (ed) The Petroleum Geology and Resources of Malaysia. Petroliam Nasional Berhad PETRONAS, Kuala Lumpur, Malaysia, ISBN: 9789839738100 Chapter 12

Moore TA, Shearer JC, Miller SL (1996) Fungal origin of oxidised plant material in the Palangkaraya peat deposit, Laimantan Tenah, Indonesia: Implications for 'inertinite' formation in coal. Int J Coal Geol 30:1–23. https://doi.org/10.1016/0166-51629500040-2

Moore TA, Ferm JC (1992) Composition and grain size of an Eocene age coal bed in southeasten Kalimantan Borneo, Indonesia. Int J Coal Geol 21:1–30. https://doi.org/10.1016/0166-51629290033-S

Morley RJ, Hasan SS, Jais JHM, Mansor A, Aripin MR, Nordin MH, Rohaizar MH (2021) Sequence biostratigraphic framework for the Oligocene to Pliocene of Malaysia: High-frequency depositional cycles driven by polar glaciation. Palaeogeogr Palaeoclimatol Palaeocol 561:110058. https://doi.org/10.1016/j.palaeo.2020.110058

Mukhopadhyay PK (1986) Petrography of selected Wilcox and Jackson group lignites from the Tertiary of Texas. In: Finkelman RB Casagrande DJ (ed) Geology of Gulf Coast Lignites. Annual Meeting of Geological Society of America, Field Trip of Coal Geology Division, pp. 126–145

Murtaza M, Rahman AHA, Sum CW, Zainey K (2018) Facies associations, depositional environments and stratigraphic framework of the Early Miocene-Pleistocene successions of the Mukah-Balingian Area, Sarawak, Malaysia. J Asian Earth Sci 152:23–38. https://doi.org/10.1016/j.jseaes.2017.11.033

Murtaza M, Rahman AHA, Sum CW (2015) The Shallow Marine Succession of Begrih Formation Pliocene, Mukah Area, Sarawak: Facies, Stratigraphic Characteristics, and Paleoenvironmental Interpretation. ICIPEG 2014. Springer, pp. 337–362

Neuzil SG, Supardi Cecil CB, Kane JS, Soedjono K (1993) Inorganic geochemistry of domed peat in Indonesia and its implication for the origin of mineral matter in coal. In: Cobb JC Cecil CB (ed) Modern and Ancient Coal-Forming Environment. Geol Soc Am Spec Pap 286:23– 84. https://doi.org/10.1130/SPE286-p23

Nugraheni RD, Chow W, Rahman AHA, Nazor SNM, Abdullah MF (2014) Tertiary coal-bearing heterolithic packages as low permeability reservoir rocks in the Balingian Sub-basin, Sarawak. Bull Geol Soc Malays 60.

O'Keefe JMK, Bechtel A, Christianis K, Dai S, DiMichele WA, Eble CF, Esterle JS, Mastalerz M, Raymond AL, Valentim BV, Wagner NJ, Ward CR, Hower JC (2013) On the fundamental difference between coal rank and coal type. Int J Coal Geol 118:58–87. https://doi.org/10.1016/j.coal.2013.08.007

Pickel W, Kus J, Flores D, Kalaitzidis S, Christanis K, Cardott BJ, Misz-Kennan M, Rodrigues S, Hentschel A, Hamor-Vido M, Crosdale P, Wagner N (2017) Classification of liptinite - ICCP System 1994. Int J Coal Geol 169:40–61. https://doi.org/10.1016/j.coal.2016.11.004

Ramkumar M, Santosh M, Nagarajan R, Li SS, Mathew M, Menier D, … Prasad V (2018) Late Middle Miocene volcanism in Northwest Borneo, Southeast Asia: Implications for tectonics, paleoclimate and stratigraphic marker. Palaeogeogr Palaeoclimatol Palaeocol 490: 141-162. https://doi.org/10.1016/j.palaeo.2017.10.022.

Shearer JC, Staub JR, Moore TA (1994) The conundrum of coal bed thickness: a theory of stacked mire sequences. J Geol 102: 611–617. https://www.jstor.org/stable/30068560.

Sia SG, Abdullah WH, Konjing Z, John J (2019) Floristic and climatic changes at the Balingian Province of the Sarawak Basin, Malaysia, in response to Neogene global cooling, aridification and grassland expansion. CATENA 173:445–455. https://doi.org/10.1016/j.catena.2018.10.044

Sia SG, Abdullah WH, Konjing Z, Koraini AM (2014) The age, palaeoclimate, palaeovegetation, coal seam architecture/mire types, paleodepositional environments and thermal maturity of syn-collision paralic coal from Mukah, Sarawak, Malaysia. J Asian Earth Sci 81:1–19. https://doi.org/10.1016/j.jseaes.2013.11.014

Sia SG, Abdullah WH (2011) Concentration and association of minor and trace elements in Mukah coal from Sarawak, Malaysia, with emphasis on the potentially hazardous trace elements. Int J Coal Geol 884:179–193. https://doi.org/10.1016/j.coal.2011.09.011

Sia SG, Abdullah WH (2012a) Enrichment of arsenic, lead, and antimony in Balingian coal from Sarawak, Malaysia: Modes of occurrence, origin, and partitioning behaviour during coal combustion. Int J Coal Geol 101:1–15. https://doi.org/10.1016/j.coal.2012.07.005

Sia SG, Abdullah WH (2012b) Geochemical and petrographical characteristics of low-rank Balingian coal from Sarawak, Malaysia: Its implications on depositional conditions and thermal maturity. Int J Coal Geol 96–97:22–38. https://doi.org/10.1016/j.coal.2012.03.002

Sia SG, Dorani J (2000) Evaluation of Coal Resources of the Mukah Coalfield, Sarawak, Malaysia, Minerals and Geoscience Department, Sarawak, GSKL 002/ 10/148, 49 p. unpublished.

Singh MP, Singh PK (1996) Petrographic characterization and evolution of the Permian coal deposits of the Rajmahal Basin, Bihar, India. Int J Coal Geol 29:93–118. https://doi.org/10.1016/0166-51629500005-4

Singh MP, Shukla RR (2004) Petrographic characteristics and depositional conditions of Permian coals of Pench, Kanhan, and Tawa Valley Coalfields of Satpura Basin, Madhya Pradesh, India. Int J Coal Geol 59:209–243. https://doi.org/10.1016/j.coal.2004.02.002

Singh PK, Singh MP, Singh AK (2010) Petro-chemical characterization and evolution of Vastan Lignite, Gujarat, India. Int J Coal Geol 82:1–16. https://doi.org/10.1016/j.coal.2010.01.003

Smyth M (1984) Coal microlithotypes related to sedimentary environments in the Cooper Basin, Australia. IAS Spec Publ 7:333–347. https://doi.org/10.1002/9781444303797.ch19

Súarez-Ruiz I, Flores D, Filho JGM, Hackley PC (2012) Review and update of the applications of organic petrology: Part 1, geological applications. Int J Coal Geol 99:54–112. https://doi.org/10.1016/j.coal.2012.02.004

Supardi, Subekty AD, Neuzil SG (1993) General geology and peat resources of the Siak Kanan and Bengkalis Island peat deposits, Sumatra, Indonesia. In: Cobb JC Cecil CB (ed) Modern and Ancient Coal-Forming Environment. Geol Soc Am Spec Pap 286: 45–62. https://doi.org/10.1130/SPE286-p45.

Sýkorová I, Pickel W, Christanis K, Wolf M, Taylor GH, Flores D (2005) Classification of huminite - ICCP System 1994. Int J Coal Geol 62:85–106. https://doi.org/10.1016/j.coal.2004.06.006

Taylor GH, Teichmüller M, Davis A, Diessel CFK, Littke R, Robert P (1998) Organic Petrology. Gebrqder Borntraeger, Berlin-Stuttgart, 704 pp.

Teichmüller M (1989) The genesis of coal from the viewpoint of coal petrology. Int J Coal Geol 12:1–87. https://doi.org/10.1016/0166-51628990047-5

Visser WA, Crew WE (1950) Stratigraphy of Teres-Penipah-Balingian Area, Sarawak. Sarawak Shell Oilfield Limited, GSKL 111/5. Unpublished.

Wolfenden EB (1960) The geology and mineral resources of the Lower Rajang Valley and adjoining areas, Sarawak. Geol Surv of British Borneo Mem 11:167